NASA CONTRACTOR REPORT

NASA CR-700

NASA CR-700

GFO PRICE $ _____

C S I PRICE(S) $ __2.50__

___ ___ __ _____

_____ __1.30__

FACILITY FORM 902

N67-15669
(ACCESSION NUMBER)   (THRU)

63
(PAGES)   /
                                   (CODE)

CR-700
(NASA CR OR TMX OR AD NUMBER)   3/
                                 (CATEGORY)

PASSIVE GEODETIC SATELLITE CANISTER ASSEMBLIES

by James O. Gibson and Robert R. Carman

Prepared by
GOODYEAR AEROSPACE CORPORATION
Akron, Ohio
for Langley Research Center

NATIONAL AERONAUTICS AND SPACE ADMINISTRATION • WASHINGTON, D. C. • JANUARY 1967

PASSIVE GEODETIC SATELLITE CANISTER ASSEMBLIES

By James O. Gibson and Robert R. Carman

Distribution of this report is provided in the interest of information exchange. Responsibility for the contents resides in the author or organization that prepared it.

NATIONAL AERONAUTICS AND SPACE ADMINISTRATION

CONTENTS

FIGURES

Figure No.

TABLES

PASSIVE GEODETIC SATELLITE CANISTER ASSEMBLIES

By James O. Gibson and Robert R. Carman

SUMMARY

The passive geodetic satellite (PAGEOS) canister assemblies were designed, analyzed for structural integrity and thermal stability, fabricated in quantities of five units, and tested for conformance to the design parameters.

The testing program required that components and materials, not previously qualified for the PAGEOS environmental conditions specified, must be tested to sufficient levels to prove their integrity.

The pre-prototype (Canister Assembly No. 1) was used for static structural testing. The prototype (Canister Assembly No. 2) was used for dynamic and thermal testing to the qualification levels of the launch and trajectory-to-orbit environmental conditions. Satisfactory completion of the qualification tests was required as a prerequisite to fabrication of the flight canister assemblies.

A high reliability was desired for the flight canister assemblies. Therefore, a thorough program of reliability analysis, monitoring of design and procurement drawings and specifications, as well as failure reporting and canister analysis, was implemented. To ensure high reliability, a quality assurance program was implemented to maintain a tight surveillance during the fabrication and testing of in-house hardware and during receipt and testing of procured hardware.

The technical requirements of the canister assembly, as shown in Design Parameters, were met by the spacecraft.

INTRODUCTION

The satellite, known as PAGEOS I, was launched into earth orbit on 23 June 1966, by the NASA Langley Research Center in support of the National Geodetic Satellite Program. It was placed in a near polar, circular orbit with an altitude of approximately 4,250 kilometers (2,640 miles) by a Thrust-Augmented Thor-Agena-D launch vehicle from the Western Test Range. This satellite is a passive, specular, solar reflector which will be used for a minimum five-year period in the measurement of the shape and size of the earth and the position of the land masses on the earth.

The 100-foot diameter, aluminum-coated spherical satellite is observed from the ground as a point source of light while it reflects the incident sunlight. Simultaneous photographs of this light source, taken against the star background by two or more widely separated ground-based cameras, will enable geodesists to determine the spatial coordinates of each camera position. An interconnected series of established camera positions will cover the entire surface of the earth, thereby permitting geometric determination of each camera position within a single reference system. It is expected that these determinations can be made to an accuracy of one part in 500,000 or 32 feet in 3000 miles.

The PAGEOS space vehicle consists primarily of a launch vehicle, a spacecraft and a shroud. The canister assembly, in its flight configuration, provided the direct means of adapting the inflatable sphere to the Agena-D vehicle, conveying it into orbit and for releasing it to permit its inflation in space at the proper time. The concept of the canister utilized the technologies developed in the Echo I and Echo II projects. The first canister assembly, designated the pre-prototype, was subjected to developmental tests, utilized in the canister ejection and canister opening tests, and was hydrostatically tested. The second canister assembly, designated the prototype, was used for the qualification tests and used in conjunction with an inflatable sphere assembly in the vacuum chamber test at Langley Research Center (LRC). The three remaining canister assemblies were to be used as flight items or spares.

The terms and items discussed in this final report are defined as follows:

Canister. - The spherical container in which the inflatable sphere assembly is enclosed.

Adapter. - The transition section which attaches the canister to the shroud support ring and the thrust face of the Agena-D.

Canister assembly. - The canister, adapter and all attachments to the canister and/or adapter.

Spacecraft. - All items above the thrust face of the Agena-D except the shroud and the shroud mount ring.

Canister ejection system. - The system utilized to separate the canister from the adapter.

Canister opening system. - The system utilized to separate the hemispherical canister halves.

Shroud. - Jettisonable fairing to protect spacecraft during ascent into orbit.

Shroud mount ring. - Ring which mounts between thrust face of Agena-D and spacecraft, on which the shroud mounts.

Inflatable sphere assembly. - That portion of the spacecraft contained within the canister during ascent, consisting of the inflatable sphere and its inflation compound.

Aerospace ground equipment (AGE). - The equipment necessary for the transportation, handling, monitoring, maintenance, repair, preparation, checkout, and assembly of the spacecraft or its components.

Launch vehicle. - All items below the shroud mount ring, which consists of a Thrust-Augmented Thor first stage with an Agena-D second stage.

Space vehicle. - The complete launch configuration including the launch vehicle, the spacecraft, and the shroud.

SYMBOLS

A	area - ft^2
a	albedo
c/c_c	ratio of systems damping factor to systems vertical damping factor
C_p	specific heat - Btu's/lb-°F
C_s	solar constant - Btu's/hr-ft^2
E	earth radiation - Btu's/hr-ft^2
F	view factor
g	gravity constant - ft/sec^2
H	altitude - nautical miles
h	adapter height - ft
i	ith node
j	jth node
K	thermal conductivity - Btu's/hr-ft-°F
L	distance or length - ft
$\bar{N}$	normal vector
$\bar{P}$	planet vector

$\dot{q}$	heat flux - Btu's/hr-ft^2
RP	radius of earth - nautical miles
RC, RL, RJ1, RJ2, RJ3	resistors - Btu's/hr-°F
$\overline{S}$	solar vector
T	temperature - °R
U	velocity - ft/sec
W	weight - lbs
x	coordinate in direction of flight
y	coordinate in right handed system
z	coordinate in direction toward earth
α	solar absorptance
α'	thermal diffusivity - ft^2/hr
β	angle between $\overline{N}$ and either $\overline{S}$ - radians
γ	angle between $\overline{N}$ and $\overline{P}$ - radians
$\triangle$	increment
δ	thickness - ft
ϵ	emissivity
θ	angle (adapter) - degrees or radians
ξ	angle (canister) - degrees or radians
π	constant
ρ	density - lbs/ft^3
σ	Stefan Boltzmann constant - Btu's/ft^2/hr/°R^4
τ	time - hours
ϕ	angle - earth - sun - radians

Subscripts:

a   aerodynamic

E   earth radiated

o   sea level

p   projected

r   reflected

s   solar

∞ free stream

∇^2 Laplacian operator

DESCRIPTION OF CANISTER ASSEMBLY - DESIGN

Introduction

The canister assembly breaks down into five major items: (1) canister, (2) adapter, (3) canister ejection system, (4) canister opening system, and (5) the instrumentation and electrical system.

The canister assemblies were designed to be compatible with the Thrust Augmented Thor (TAT) Agena-D vehicle. Relative to the aerodynamic shroud, it was determined that (1) the canister assembly cleared the specified static and dynamic clearance envelope for the shroud, (2) the adapter section of the canister assembly accommodated the wire routing required for the shroud instrumentation and shroud functions, and (3) the canister assembly was designed such that after installation of the shroud, all operations required on the spacecraft were affected through one 6-3/8-inch diameter hand hole and a 2-inch diameter observation port in the shroud. The lower ring was machined in one piece with a closed-angle cross section and provided an eight bolt pattern with a rotational positioning index pin clearance hole for mounting the spacecraft to the shroud mount ring. Relative to the Agena-D vehicle, the canister assembly was designed to survive the flight environment with a high degree of confidence, to accommodate the specified connectors and connector locations on the Agena diaphragm that were used for the canister instrumentation and the canister ejection system pyrotechnics wiring.

A PAGEOS spacecraft, complete with thermal control coating, is shown in Figure 1. The canister assembly configuration and canister assembly general arrangement are illustrated in Figures 2, 3A and 3B respectively.

Canister

The canister (a spherical pressure vessel with an inside diameter of 26.5 inches) contained and protected the inflatable sphere from the time of packaging, through launch, to deployment. In principle, it is the same as the Echo I canister. The halves were machined from two hemispherical magnesium forgings (ZK60A-T5), and interconnected at the equator.

The canister halves were mated at the equator as shown in Figure 4. Each half was machined circumferentially at the equator to provide a sliding valve for control of shaped-charge debris and to support the canister halves structurally. A thin neoprene vacuum-tight face seal was bonded to each canister half. The seals were lubricated with a high-vacuum grease before the canister was closed and maintained the vacuum inside the canister. A dove-tailed ring groove in the male wall accommodated an "O" ring as part of the canister opening system. The halves were laced together by cord passing through holes drilled through the external equatorial flanges of each canister half. These flanges also contained holes for handling and packaging with aerospace ground equipment.

The external equatorial flanges and the sliding valve design were dictated by the canister opening system. The external flanges entrapped and positioned the shaped-charge for the canister opening system and absorbed and distributed the explosive forces of the shaped-charge required to impart a minimum velocity of 20 fps to each canister half. The design of these flanges, and their transition to the canister wall, was a critical item of detail design. The sliding valve was designed to prevent shaped-charge debris from passing through the joint and impinging on the packaged sphere. The diametrical clearance on the sliding valve is held to from 0.002 inch minimum to 0.008 inch maximum. The sliding valve surfaces were treated with a dry film lubricant to maintain low friction on all mating surfaces.

The upper canister half had a thicker wall (0.108 ± 0.005 inch) than the lower half (0.065 + 0.005 inch) so that the weights were approximately equal and the energy of the shaped-charge detonation reacted on approximately equal masses and thus imparted approximately equal velocities to each half.

Two solenoid operated canister valves, with removable fiberglass covers, were mounted 180 degrees apart just above the equatorial flange of the canister upper half as shown in Figure 4. These valves were the normally-closed type and were used in conjunction with aerospace ground equipment for canister pressure regulation.

The lower canister half had three ports, two just below the equatorial flange (see Figure 4) and one adjacent to the lower pole, which accommodated the installation of pressure transducers. These too were faired with removable fiberglass covers.
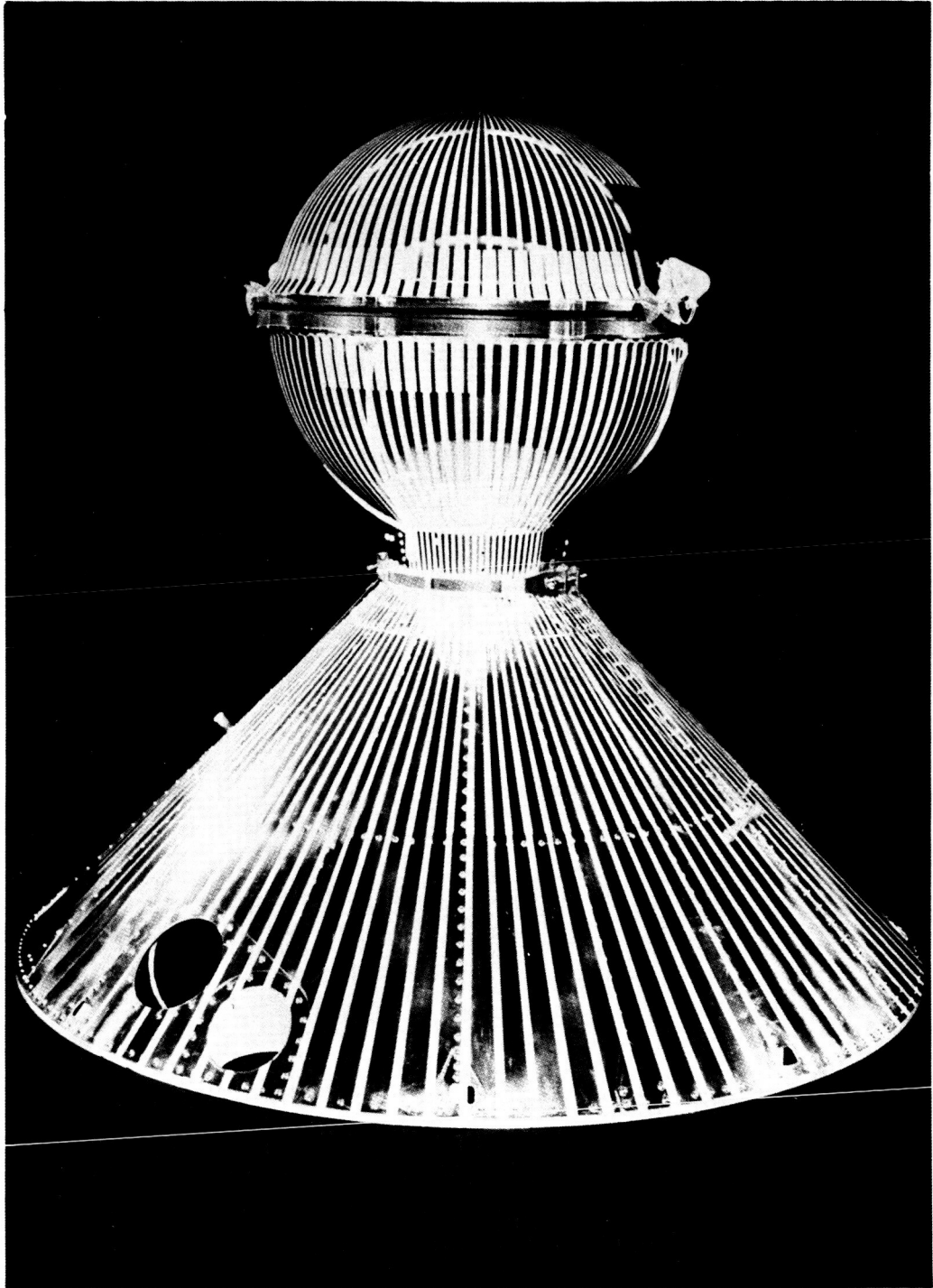
Figure 1. - PAGEOS spacecraft.

SECTION AA
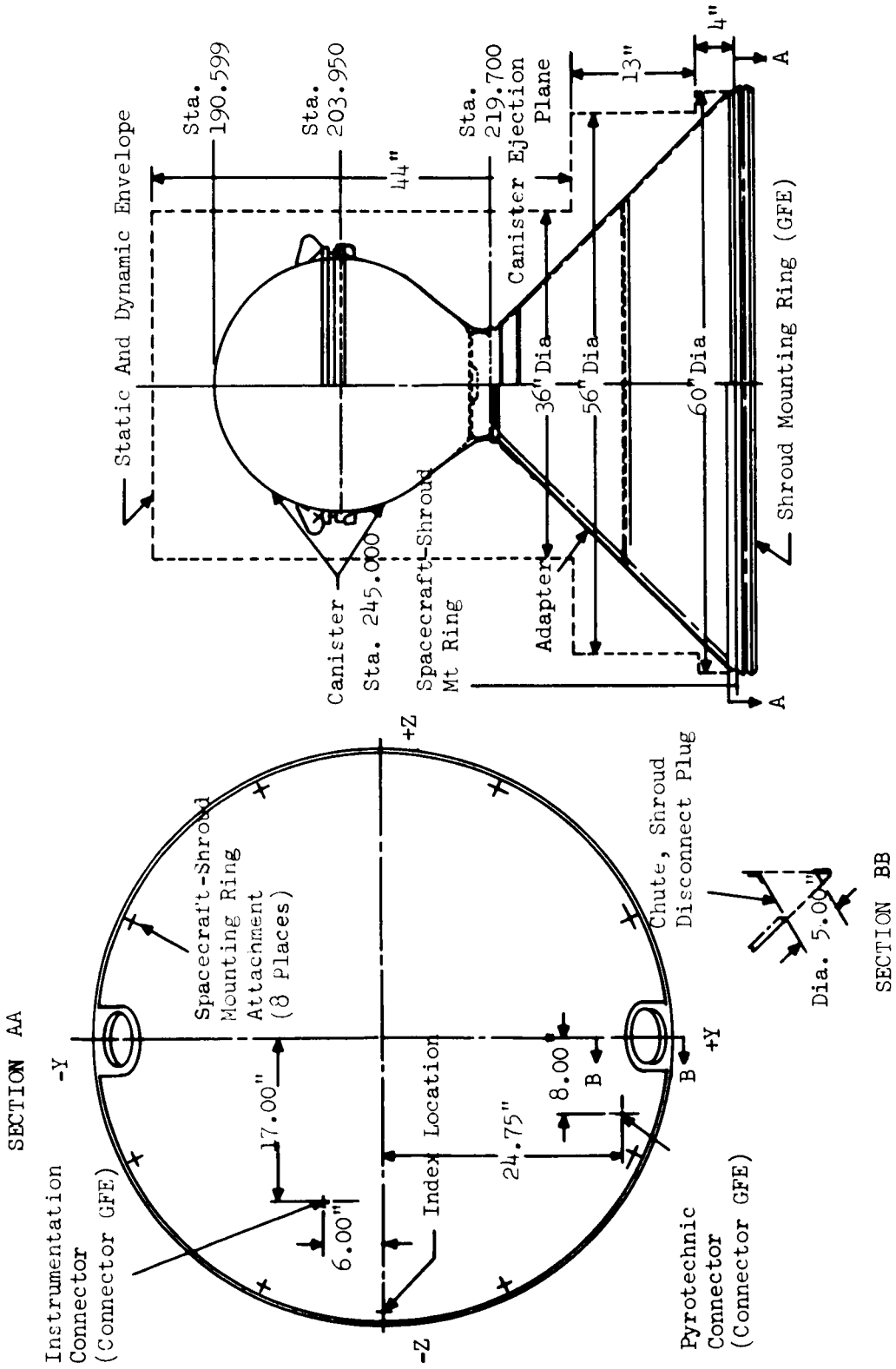
Figure 2. Canister assembly configuration

8

Transducer, Temp

Lacing

F.L.S.C.

Canister

Solenoid
Valve

Solenoid
Valve

Sta 203.950

Pressure
Trans.(Flight)

Pressure Trans.
(Flight and AGE)

Spring
Ejection
System

Transducer
Temp

A

A

Sta 219.700
Canister Ejection Plane

Box, Canister
Instrumentation

Converter,
Power

Adapter

Sta 245.000
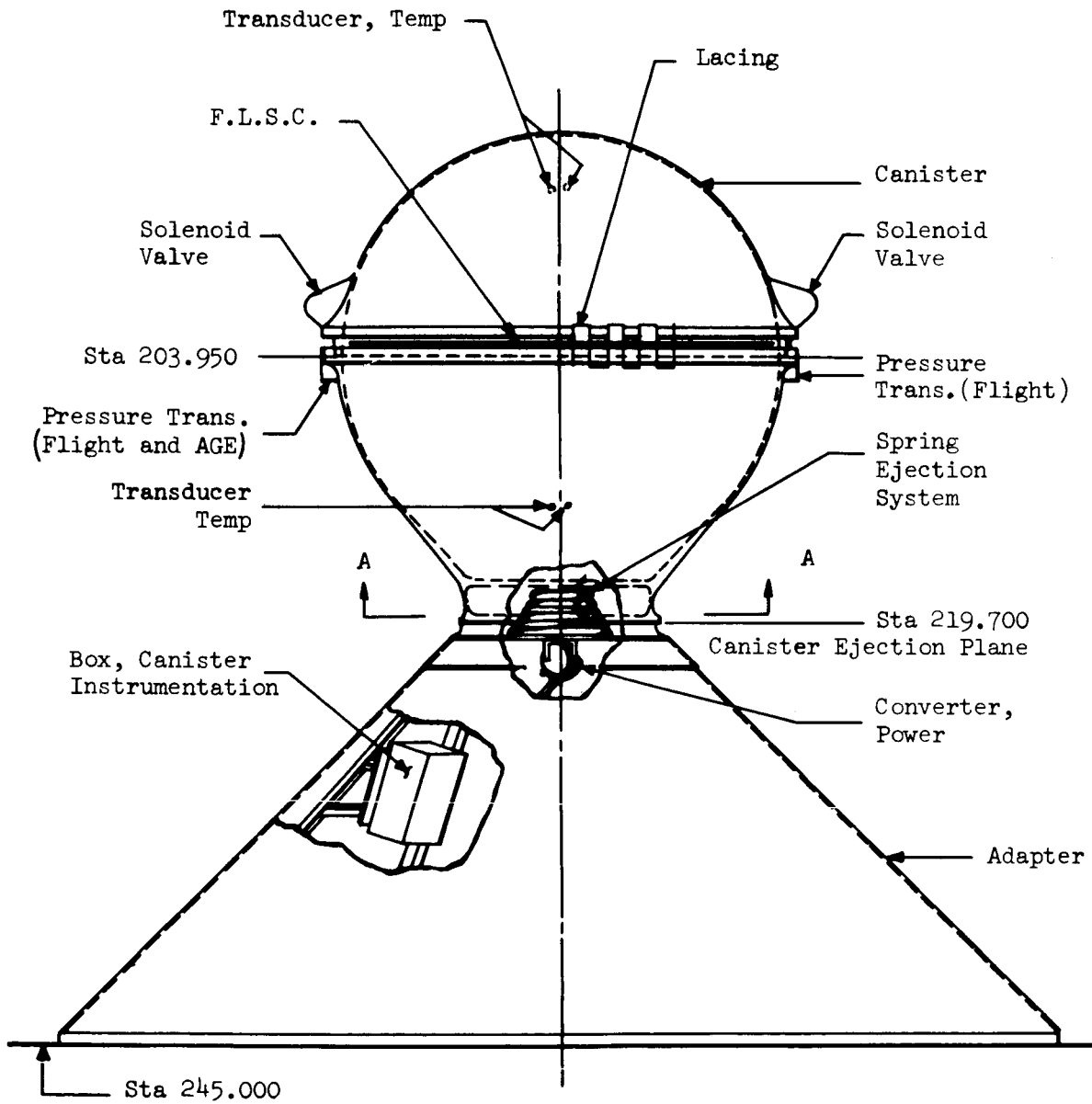
Figure 3A. - Canister assembly general arrangement.

Detail A-A
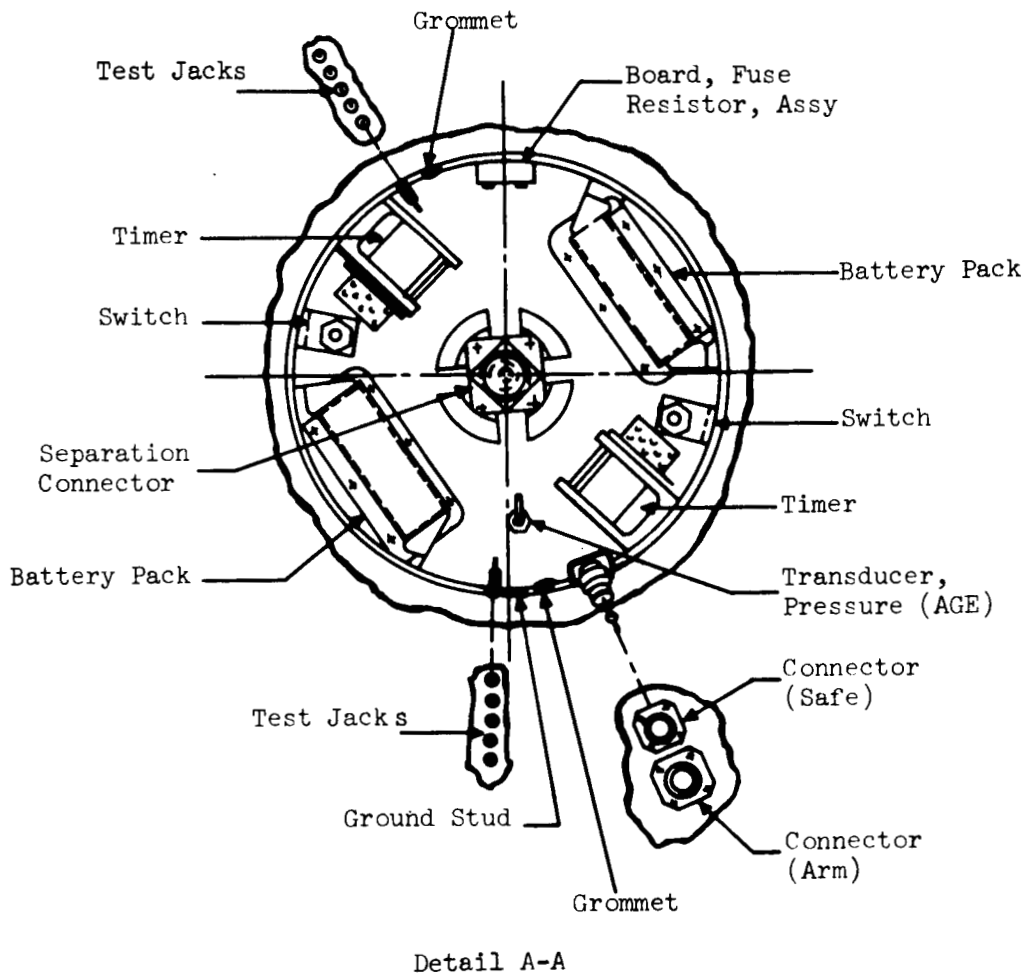
Figure 3B. - Canister assembly general arrangement

Removable
Cover

Cap

Canister
Upper Half
(Male)

Evacuation
Valve

Gauze

Lacing
Holes

"O" Ring

Face Seal (2)

Pressure
Transducer

Gauze

Canister
Lower Half
(Female)

Figure 4. - Canister mating.

Explosive
Bolts

Quick Release
Clamp

Canister

Ejection Spring

Adapter
Upper Ring

Seat

Station
218.4

Adapter

Breakaway Electrical
Connector

Retainer

Lanyard

Figure 5. - Canister to adapter mating and ejection system.

Two pairs of temperature tranducers (one of each pair redundant) were mounted on the canister to monitor both the highest and lowest temperatures encountered by the canister during flight. Two of the interchangeable transducers were installed in the upper canister half and two in the bottom.

All ports inside the canister were covered with gauze pads and the entire surface of the canister coated with Emeralon 320 (0.2 to 0.7 mil thick) to minimize abrasion of the inflatable sphere.

The canister was mounted to the adapter at the pole of the lower half (see Figure 5). A hollow conical section approximately 11 inches in diameter (an integral part of the machined magnesium forging) extended approximately 3.5 inches to the adapter mounting surface. Provisions were made in this section for mounting of the switches, timers, and battery packs and the plug for the canister opening electrical system and AGE monitoring of spacecraft flight functions. A tapered seat in the conical canister extension and adapter respective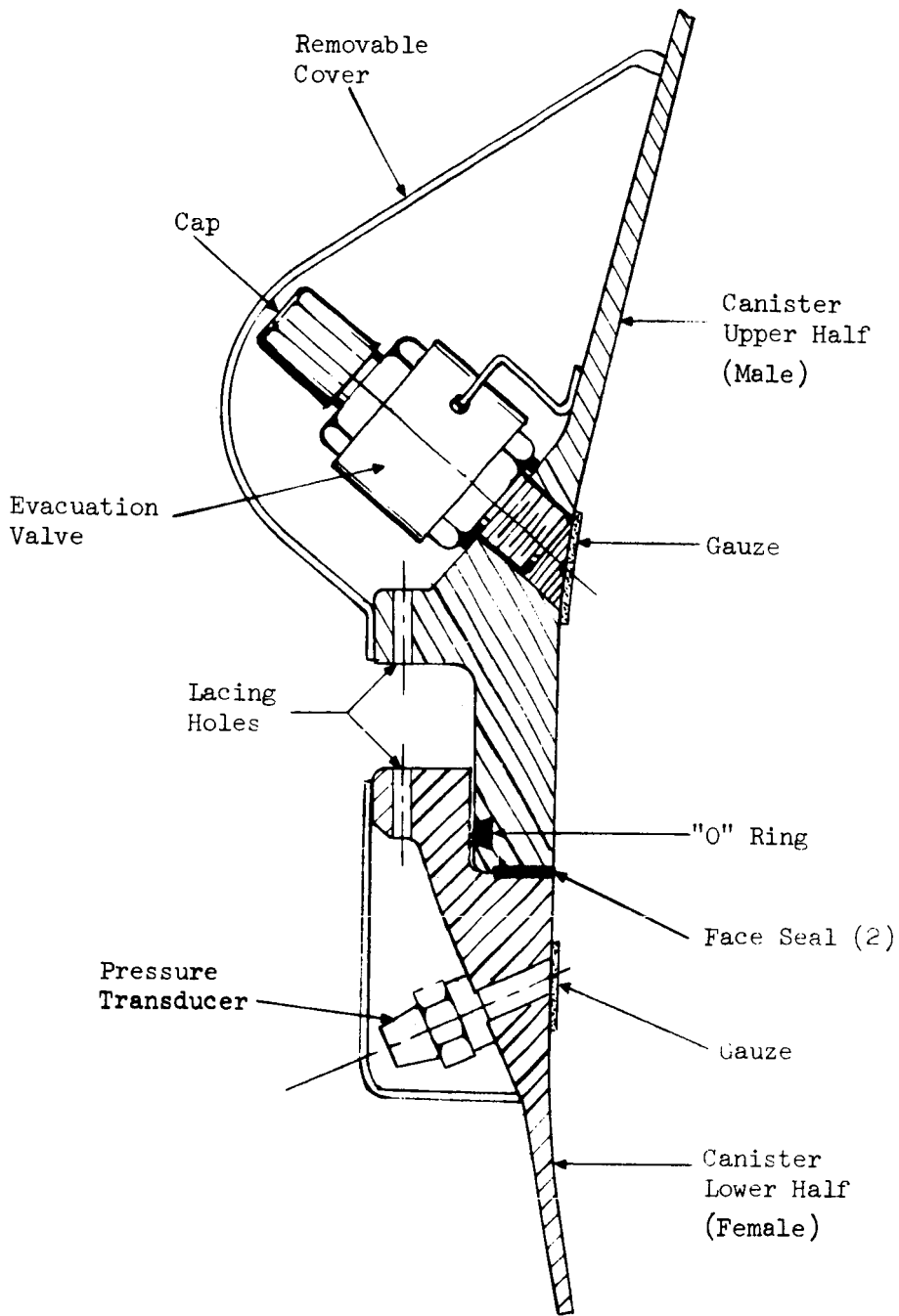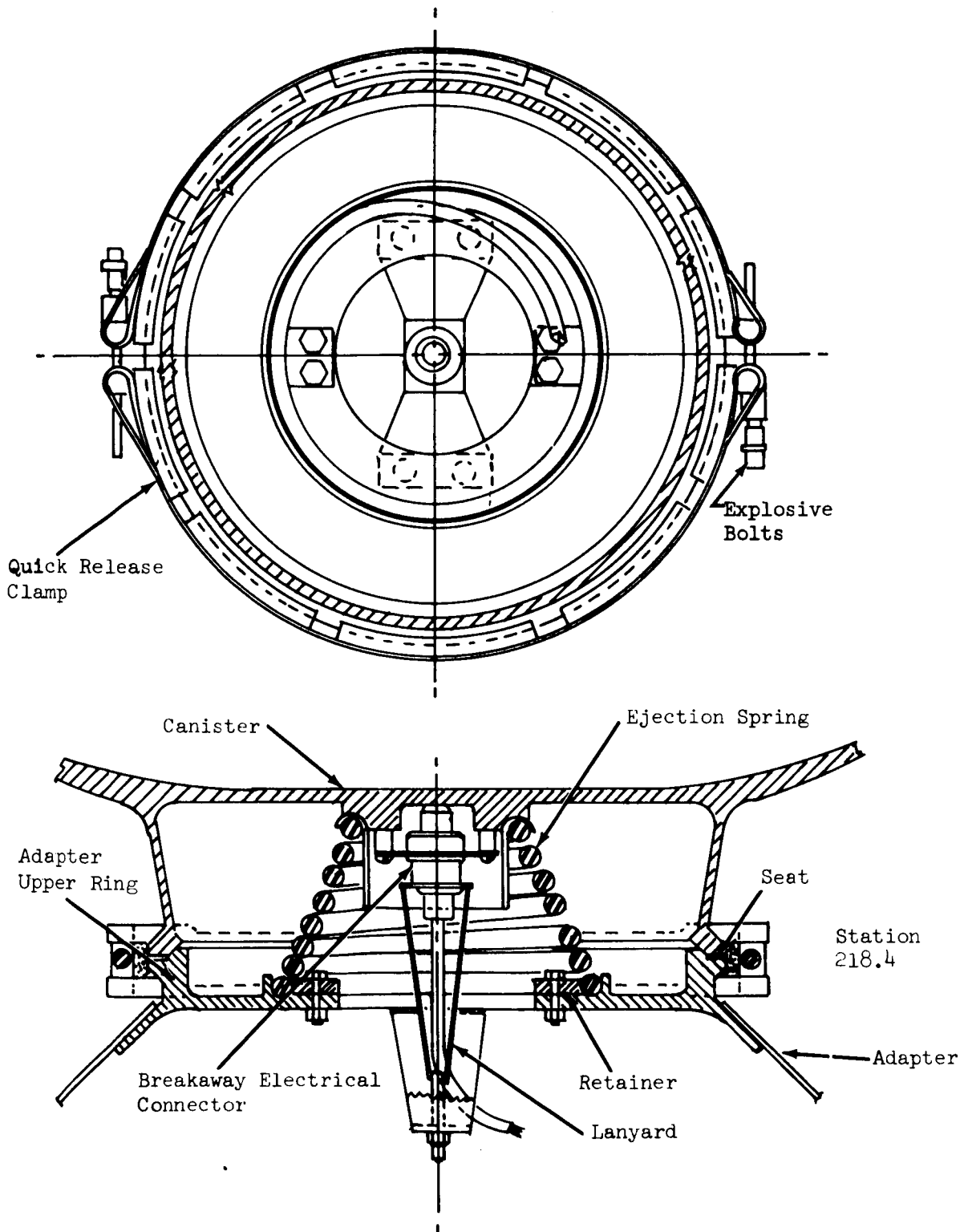ly, structurally indexed the mating parts, and a spherical detent provided rotational indexing. The mated parts were held together by a quick-release type clamp that gripped external machined V flanges.

The ejection system spring and the electrical wiring that transmitted the canister temperature and pressure data to the Agena telemetry system were installed inside the hollow conical section (see Figure 5). An external boss was machined into the canister shell to provide the register for the ejection spring. Undercuts in the boss permit routing of the instrumentation wiring to a rigid aluminum conduit mounted on the center line of the canister. This conduit was attached to the canister lower half by screws in tapped holes in the boss; it provided the support for the breakway plug required at the ejection plane.

The exterior surface of the canister was provided with a thermal control coating which consisted of an inorganic finish (white epoxy enamel), 5 to 10 mils thick, applied to the entire exterior surface, which was then partially covered with a pattern of 0.002-inch thick, aluminum foil, pressure sensitive thermal reflective tape.

Adapter

The adapter was a frustum of a 45° (half-angle) cone approximately 25.5 inches high with a base diameter of 60 inches. The upper and lower surfaces mated the respective structural-mechanical interfaces with the canister and shroud mount ring. A semimonocoque construction was utilized consisting of an 0.032 inch aluminum skin riveted to a framework of two machined circumferential aluminum rings (upper and lower) and one intermediate aluminum sheet metal ring interconnected by 16 aluminum angles along element lines of the cone. The two-piece skin was butt spliced 180° opposed on flanges of two of the sheet metal angles. An intermediate riveted structure accommodated mounting of the electrical instrumentation box.

The upper ring provided the mounting surface for the canister as defined in the canister description and shown in Figure 5. It also supported and position-indexed the canister ejection spring and maintained the canister opening-start switches (mounted in the canister) in the circuit-open positions until the canister-ejection signal occurred.

Access to the two electrical connectors at the Agena diaphragm was provided through two doubler-reinforced hand holes in the skin. Two 5-inch diameter chutes, 180° apart, were provided through the skin structure to accommodate shroud instrumentation and shroud functions wiring.

The exterior surface of the adapter was provided with a thermal control coating identical to that of the canister, which consisted of 5 to 10 mil thick inorganic finish (white epoxy enamel) applied to the entire external surface which was then partially covered with a pattern of pressure sensitive aluminum foil, 0.002-inch thick, thermal reflective tape.

Canister Ejection System

The ejection system, upon receipt of firing current from the Agena-controlled signal, released the canister from the adapter and ejected it from the space vehicle at a minimum relative velocity of approximately 6 fps. At the same time, switches were activated in the canister base for initiation subsequent programmed deployment events which are as follows:

(1) Connect battery voltage to timer dimple motors.

(2) Firing of dimple motors unlatched and started the spring wound primary and secondary timers.

(3) At rundown of timers the battery voltage is connected to the detonators for the shaped charge initiation.

The mechanical components of the ejection system were (1) an ejection spring, (2) a quick-release clamp connecting the canister and adapter, and (3) explosive bolts for clamp release. (The electrical system is discussed under the Instrumentation and Electrical System description.)

The conically wound ejection spring was installed under compression and imparted the relative velocity to the mass of the canister when the canister-adapter clamp was released. The spring, made from ASTM type 6150 steel wire, was attached to the adapter and compressed between the canister and adapter and position-indexed symmetrically around the vertical center line.

The quick-release clamp was made in two halves connected by two explosive bolts. Each half was attached to the adapter with three lanyards. The clamp was a flat stainless-steel band with V-index blocks attached to and locally spaced around the inside surface of the band. These blocks registered with the mated external V flanges at the canister-adapter interface.

Each clamp band terminated at a machined end trunnion. Clearance between the end trunnions of the respective clamp quadrants permitted tensioning of the clamp bands. In addition to the redundancy provided for firing the explosive bolts, (as explained in Instrumentation and Electrical System), the clamp design permitted complete release of the clamp with only one bolt firing. The contact and release surfaces, the clamp V blocks with the V flanges, and the canister base with adapter seat, were treated with a dry film lubricant to reduce friction on all release surfaces.

Canister Opening System

The canister opening system interconnected the canister halves. On receipt of a signal, it released the halves and imparted a minimum velocity of 20 fps to each. The mechanical components of the canister opening system consist of (1) a shaped charge, (2) strux, (3) an "O" ring, (4) lacing, (5) rubber liners, and (6) shaped-charge thermal protection cover. The canister opening mechanical system is shown in Figure 6.
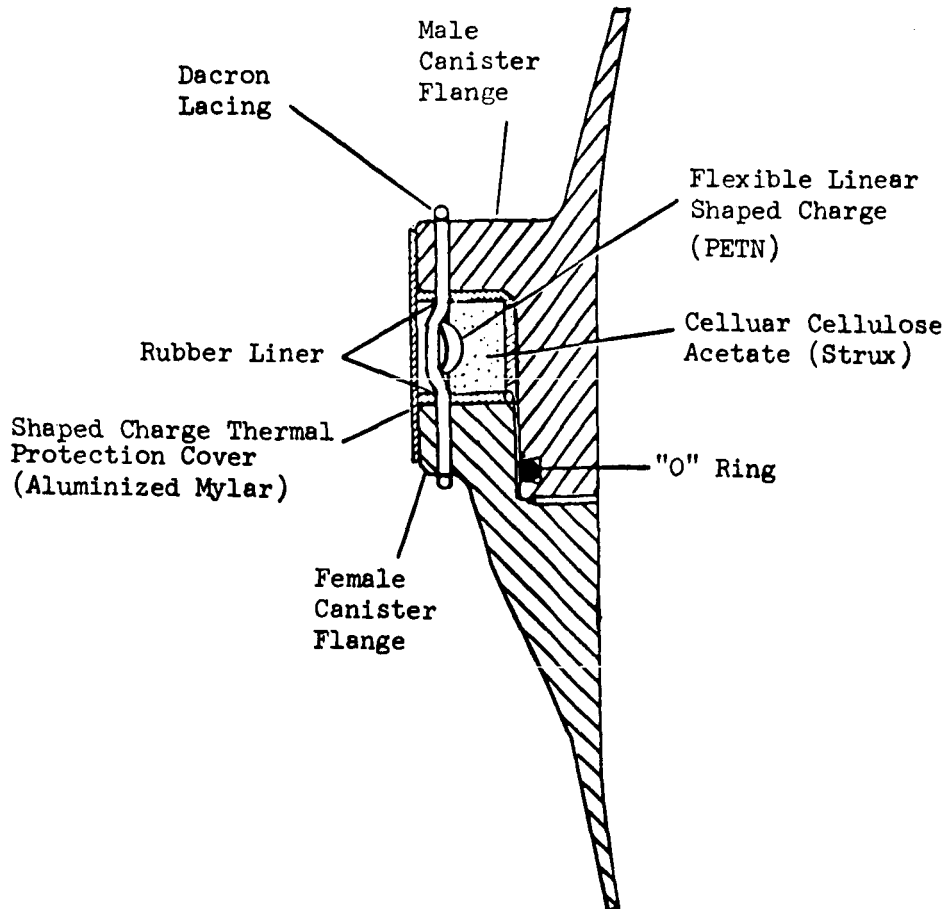

Figure 6. - Canister opening system.

The shaped charge was a nominal 40 grain per foot, lead-encased cresent-shaped PETN flexible linear charge. Its concave side faced the lacing and cut it at initiation. The high-detonation propagation rate of the charge applied an impulse to the equatorial flanges of the canister halves and opened the canister. A primary and backup detonator were used to initiate the shaped charge. They were installed through holes in the lower canister equatorial flange. The lower ends of these holes were tapped for the detonator retainer and the upper ends contained steel bushings that prevented the flange from splitting when the detonator was fired. The detonators were secured in direct contact with the shaped charge. Removable fiberglass covers faired and protected each detonator installation. Strux, a cellular cellulose acetate, was machined to precise dimensions required to mount and preposition the shaped charge in the center of the equatorial flange gap.

The lacing interconnected the canister halves and also held the shaped charge and Strux in place. It was pretensioned Dacron line, laced through holes in the equatorial flanges of the canister halves. The holes were chamfered to prevent fraying or cutting of the lacing. The lacing was installed in short segments so that failure of one segment would not permit premature opening of the canister under external vacuum conditions.

Rubber liners were bonded to the shaped charge side of each equatorial flange to minimize damage to the flanges when the shaped charge was exploded. Half mil aluminized Mylar tape, attached with a pressure sensitive adhesive to the canister flanges, covered the space between the equatorial flanges of the canister halves to provide thermal protection for the shaped charge.

Instrumentation and Electrical System

Overall considerations. - The spacecraft instrumentation and electrical system is shown in Figure 7. It provided all electrical connections within the spacecraft, the electrical connection for launch vehicle command functions, telemetry data, power supply, and monitoring circuitry. The system was composed of the following: (1) canister instrumentation for monitoring of pressure and temperature, (2) canister ejection, and (3) canister opening.

The entire PAGEOS instrumentation system power input was 0.332 amperes from the Agena-D regulated 28 VDC power supply. The load was continuous prior to and during the launch period. The data signals were conditioned by spacecraft instrumentation so that 0 to 5 V (± 2%) corresponded to a pressure range of 0 to 10 torr (± 2%) and a temperature range of -10 to +200°F (± 2%). The canister ejection monitor signal was a step-change in voltage from 2.13 to 4.0 volts (± 0.03 V) at canister ejection. An electrical harness was routed from the instrumentation electrical package to the Agena-D connection.
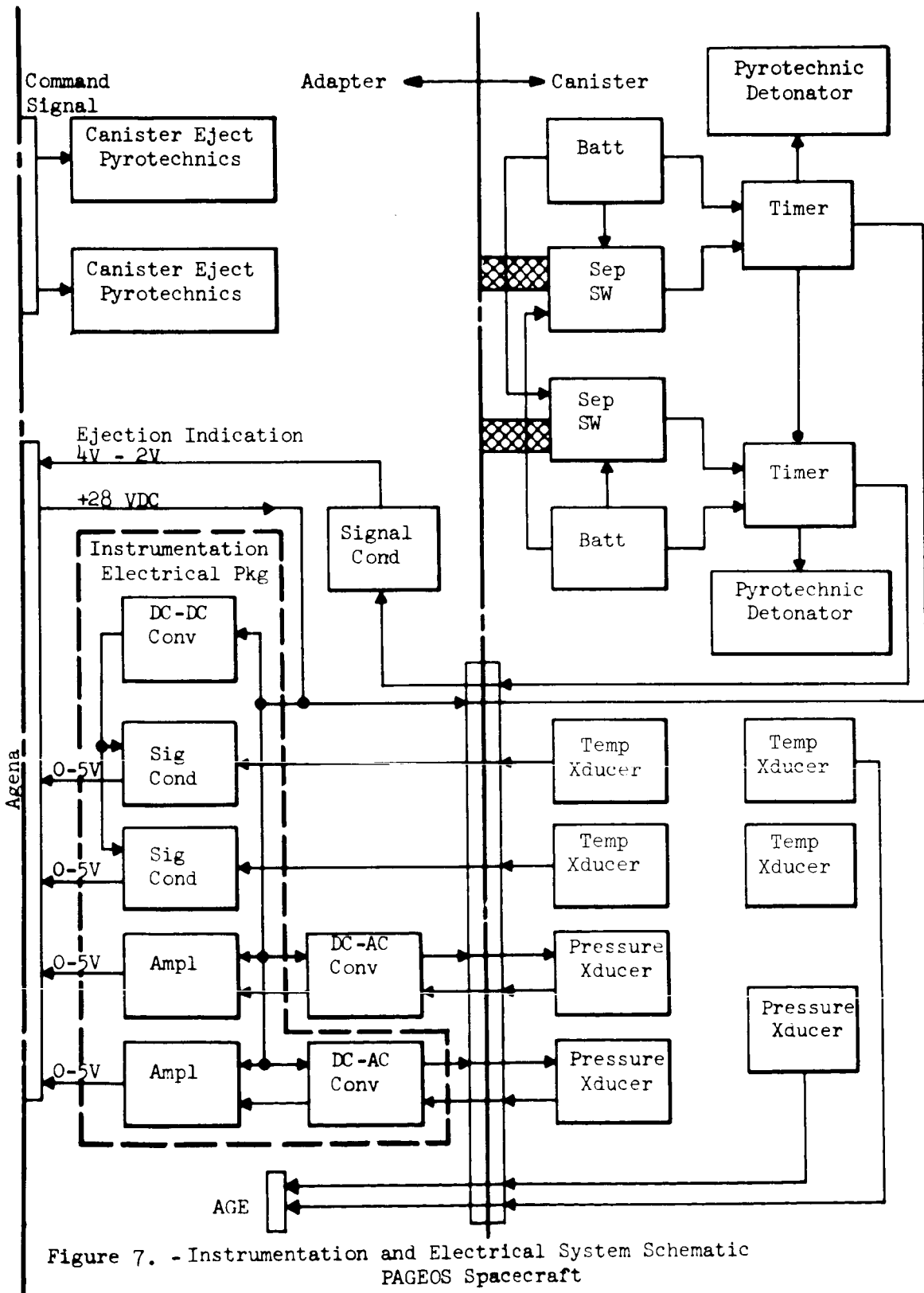
Figure 7. - Instrumentation and Electrical System Schematic
PAGEOS Spacecraft

.The canister-ejection electrical system included the initiation circuitry for the explosive power cartridges used in the explosive bolts. A separate electrical harness for this system was attached to the adapter structure. The circuits were redundant, and each power cartridge was a dual-bridge wire device.

The canister-opening electrical parts consisted of the initiation circuitry for the flexible linear shaped charge and were contained within the conical section of the canister lower half. The electrical circuits were redundant; each circuit contained a battery pack, a timer, and an initiation switch. One shaped charge detonator was included in each redundant circuit, each capable of initiating the shaped charge. An electrical harness connected the electrical components in the canister base to the shaped charge detonators. Two environmental proof initiation switches on the canister were used to close the circuit between the timer dimple motors and the battery packs, thus firing the dimple motors and starting the timer.

Canister instrumentation. - The monitoring of the spacecraft canister pressure required a highly sensitive system. Continuous monitoring of the canister pressure was required from closure to ejection. The pressure-sensing system that was selected measured the pressure accurately in the 0 to 10 torr range. It contained a pressure transducer and a subminiature power supply. The output of the transducer was conditioned by a DC amplifier that provided a signal output level and impedance compatible with the commutated subcarrier oscillator channel on the Agena-D telemetry system.

The temperature transducers on the canister were located (from trajectory analysis) to monitor both the highest and lowest temperatures encountered. The transducer leads were terminated to facilitate changing from one transducer to the other, should one become inoperative before launch. In addition, the redundant transducer on the canister lower half was wired to be used in conjunction with AGE as a canister temperature monitor prior to mating with the Agena-D. The temperature sensor was used in conjunction with signal-conditioning circuitry, which was powered by a 5.0 volt output DC-DC power converter.

The canister ejection monitor signal was obtained by opening a shunt across a voltage divider network that caused a step-voltage change from 2.13 to 4.0 volts when the canister was ejected. The shunt was wired through the canister-adapter separation connector, one contact on each timer, and back through the separation connector. This provided a telemetry indication not only of canister ejection, but also of premature initiation of the canister opening system. The canister ejection monitor system provided a continuous signal output level and impedance compatible with the Agena-D telemetry system.

All of the instrumentation systems were compatible for use with the Agena-D hardline monitoring and the Agena telemetry transmitter.

Canister ejection. - The canister ejection system was redundant in that there were two clamp separators with dual bridge wires in each explosive power cartridge with individual twisted and shielded leads for each bridge wire. The clamp separators were designed to release and impart a separation impulse to the clamp halves by utilizing gas pressure generated by a power cartridge. The gas pressure acted on a sliding piston that caused the bolts (in tension) to break at a V-groove point. The piston had approximately a 1/8-inch overtravel that imparted the separation impulse on the clamp halves. The piston employed an "O" ring seal and was retained in the assembly, thereby containing the combustion products of the power cartridge.

The power cartridge utilized was a dual bridge wire device with each bridge wire having a resistance of 1.1 ± 0.1 ohm. The power cartridge and its associated spacecraft wiring were designed with primary consideration being given to AMFTC Ordnance Standards (1 amp - 1 watt no-fire level for 5 minutes) and AMFTCP 80-2 General Range Safety Plan. The ejection command signal from the Agena-D launch vehicle, connected power to the dual bridge wires of the explosive power cartridges causing both clamp separators to release with a positive force being applied to the clamp halves causing them to separate. An additional separating force was applied to the clamp halves by virtue of their spring steel construction. Provisions for shorting and arming plugs for the pyrotechnics were supplied on the Agena-D launch vehicle.

Canister opening. - The canister opening system was sequentially redundant from ejection signal through the detonation of the pyrotechnics. Each system was energized by a switch that closed when the canister was ejected. The closing of the switch started two timing mechanisms. When the timer in the primary firing circuit timed out to 83.5 sec, the timer switch closed and applied power from the battery power pack to the shaped charge detonator located at the +Y axis. In event the primary detonator would not initiate the shaped charge, the timer in the secondary firing circuit timed out to 90.0 sec. At this time, its switch closed and applied power from the redundant battery pack to the secondary shaped charge detonator located at the -Y axis. The canister ejection signal and timer initiation device was an environmental proof switch. Timers connected the redundant battery power supplies to the bridge wires of the shaped charge detonators. These timers were spring-driven escapement-type devices activated by pyrotechnic dimple motors. They had a 90-sec total time motor preset by adjustable cams and limit switches to detonate the pyrotechnics in 83.5 and 90.0 sec, respectively. Each had two dimple motors, either of which activated the timing cycle. Each had two SPDT switches; one to connect the battery pack directly to the shaped charge detonators for opening of the canister, and the other was used to monitor the status of the timer through a continuity check prior to installation on the Agena-D launch vehicle and through telemetry after installation on the Agena. The shaped charge detonators are single bridge wire devices with a bridge wire resistance of 1.0 ± 0.1 ohm. The detonators and their associated spacecraft wiring were designed with the

same primary consideration being given as described for the power cartridge of the canister ejection system.

The dimple motors were single bridge wire devices with a bridge resistance of 0.25 to 0.45 ohm and were designed for a no-fire current level of 0.5 amp for one 30 sec pulse.

The power for the canister opening system was supplied by redundant battery packs, each containing seven silver-zinc cells connected in series. The cells were mounted in a sealed container and provided adequate power to activate the system. For safety, an "arming" and a "safing" plug were incorporated into the canister opening system. They were located on the conical portion of the lower canister in a position accessible through a hand hole in the Agena-D shroud after it was installed. When the "arming" plug is removed, the battery packs are completely disconnected from the other opening system circuitry. When the "safing" plug was installed, a shunt was placed across the shaped charge detonator bridge wires. The canister opening system was armed by removing the "safing" plug and installing the "arming" plug. Lanyards of sufficient length to reach through the hand hole in the Agena shroud and be held externally were provided on both plugs. This permitted them to be retrieved without removing the shroud in event one should be dropped inside the shroud during the arming procedure. The arming plug lanyard was cut and pulled out through the hand hole in the shroud after arming.

Ten test jacks were provided in the side of conical portion of the lower canister for checking the electrical status of the canister opening system prior to shroud installation. Four of the test jacks were provided for checking the condition of the battery pack and for charging the batteries, if necessary.

DESIGN PARAMETERS

The following parameters (constraints) were established for the design of the PAGEOS canister assemblies and the related aerospace ground equipment.

(1) Canister halves to be made from magnesium forgings.

(2) Canister to be a 26-1/2 inch inside diameter sphere.

(3) Halves to be mated at equator with sliding-valve type joint with face seals for vacuum retention.

(4) Halves to be laced together through equatorial flanges.

(5) Flexible linear shaped charge (FLSC) to be lead encased crescent shaped PETN.

(6) FLSC to be accurately centered between flanges.

(7) Flange design to prohibit impingement on the satellite of debris from explosion during opening.

(8) No cracks, breaks or serious damage permitted on flanges during opening.

(9) No sharp edges or protrusions on canister.

(10) Anti-chaffing liner required.

(11) Temperature maintained between +32°F and +140° F at all times after sphere installed.

(12) Thermal control on canister must prevent seizure of the sliding valve at time of opening.

(13) Monitor temperature and pressure at all times after closing.

(14) Provision for evacuation after canister closing.

(15) Capable of maintaining 1 torr or less with leak rate no greater than 0.1 torr per 24 hours.

(16) Canister opening system mounted on lower canister half.

(17) Two halves approximately equal weight.

(18) 20 foot/sec minimum separation velocity for heavy half in vacuum of 10^{-2} torr.

(19) Canister opening 60 sec minimum, 90 sec maximum after ejection.

(20) Canister ejection velocity of 6 feet/sec minimum.

(21) Ejection system and instrumentation shall be contained within the adapter.

(22) Adapter to be frustum of a 45 degree cone.

(23) A quick-release type clamp shall attach canister to adapter.

(24) Adapter to accommodate wiring and plugs to shroud.

(25) Spacecraft weight of 265 pounds maximum.

(26) Echo I pyrotechnics, except range safety takes precedent.

(27) Pressure transducer range 0 to 10 torr 2 percent accuracy commutated, temperature -10° F to 200° F, 2 percent accuracy commutated, separation (blip) continuous, monitor timer position during countdown and flight.

(28) All ordnance items must have shorting plugs.

(29) All category A ordnance items must be capable of being interrupted between device and power source.

(30) Canister assembly must be able to survive qualification tests without damage.

(31) Make provisions for use with AGE.

(32) Must withstand qualification, flight and handling loads.

(33) Factors of safety:
    (1) Spacecraft
        (a) FS (yield)   - 1.00
        (b) FS (ultimate) - 1.50

    (2) AGE
        (a) FS (yield)   - 1.5
        (b) FS (ultimate) - 2.0

ANALYSIS

Scope

The analysis was performed, based on the government furnished flight environmental and trajectory data. The analysis was divided into two major parts; (1) thermal, and (2) structural. A weights study, including a mass properties study, was also conducted in support of the PAGEOS project.

Thermal Analysis

This analysis covers a flight duration of approximately 72 minutes, the period from shroud ejection to canister separation. The Agena aerodynamic shroud is used to protect the canister assembly and control its temperature, so that when the shroud is ejected, the assembly is at approximately 70°F. The exposed canister assembly, starting at 70°F, must then go through a short coast and firing period of five minutes and then a 180° transfer orbit, after which it is injected into the satellite orbit.

The canister assembly was analyzed in the following sequence. First, the geometry was defined; then, the heat inputs were determined for all the modes of the canister assembly. The thermal resistors were calculated and finally the temperatures were calculated.

In calculating the temperatures, no heat transfer was included for the inside of the canister or the adapter. As a result, the temperatures from this analysis will result in higher maximum temperatures and lower minimum temperatures than would have been obtained if the internal heat transfer was included.

20°

180°
TRANSFER ORBIT
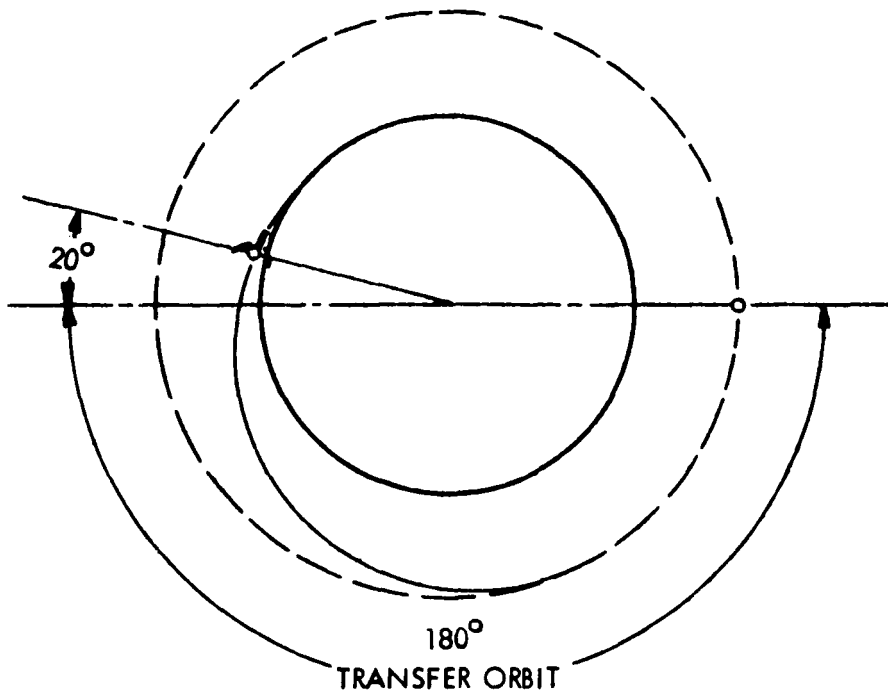
Figure 8. - Flight period covered by analysis.

The following assumptions were made:

(1)   Solar constant is 443 Btu/Hr-Sq Ft.

(2)   The Earth's albedo is 0.4 and constant.

(3)   The canister has no internal heat transfer.

(4)   The adapter had no internal heat transfer.

(5)   There is no heating from the Agena diaphragm.

(6)   The spacecraft is at 70°F when shroud separates.

(7)   The radiating earth is isothermal.

(8)   The earth is spherical and has a radius of 3492 n. mi.

(9)   The earth is a diffuse reflector.

(10) There is no temperature gradient through the skin thickness
       of the spacecraft.
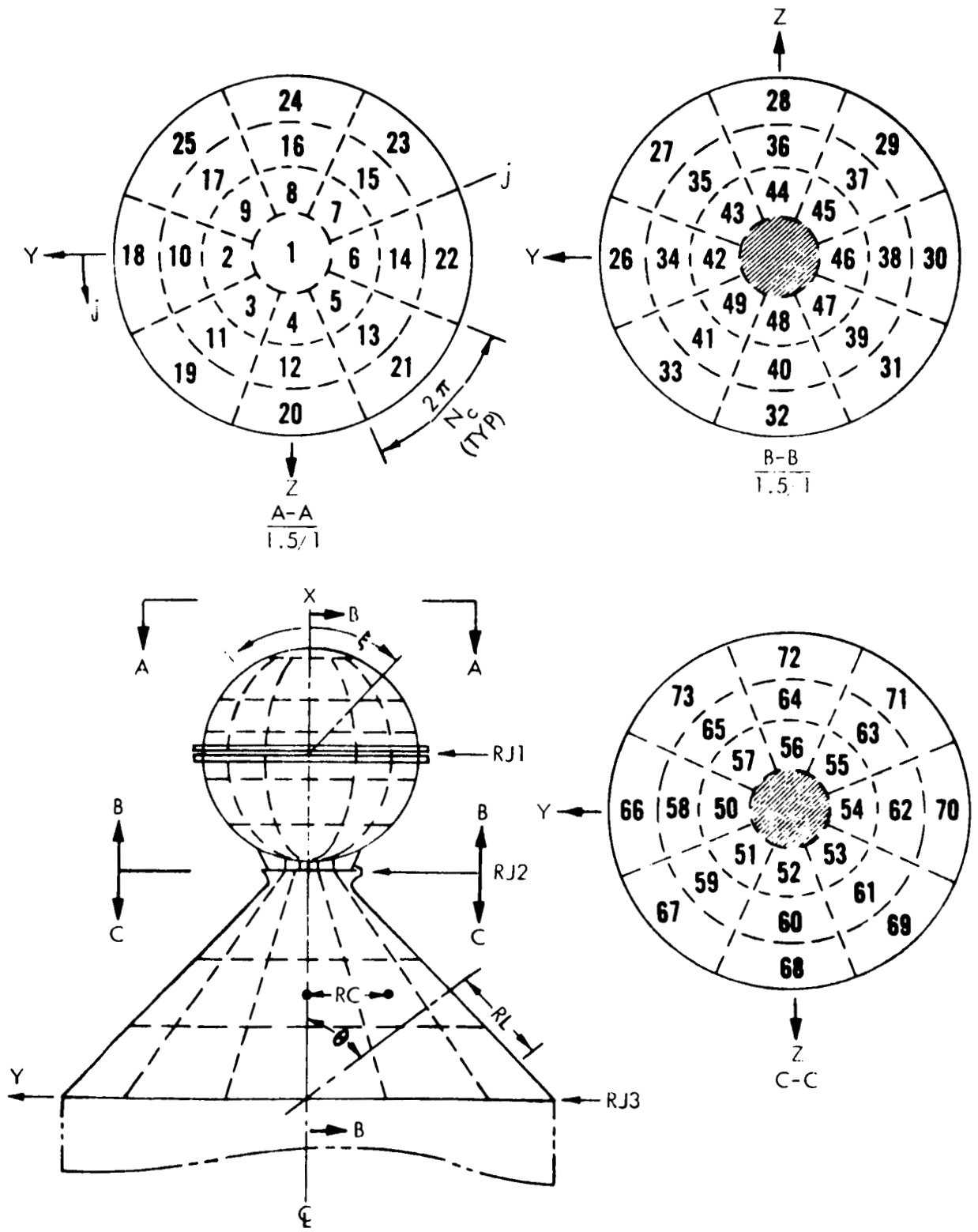
Figure 9. – Canister assembly geometry and nodes.

Analytical model. - The canister assembly unit was divided up into a number of isothermal nodes as shown in Figure 9. These were grouped into three sets of nodes; the top half of the canister, the bottom half of the canister and the adapter. All of the nodes in one set or section are considered a part of a solid homogeneous material. Each section is connected to the next section by a contact surface area having some thermal conductance. The thermal resistors at these joints, RJ1, RJ2 and RJ3 in Figure 9, are included in the model but were set at very high values so that the thermal resistance across the joints would be at the maximum.

For any node "i" during a time increment $\Delta\tau$ the heat balance would be as shown in Figure 10.

The heat flux at the surface area, $\dot{q}_{i,j}$, is for the external surface only since it was assumed that the node has an adiabatic internal surface. This net heat flux at the surface consists of two terms; the incident heat flux, q_{in} and the heat flux radiated away, $\dot{q}_{rad}$.

$$\dot{q}_{i,j} = (\dot{q}_{in} + \dot{q}_{rad})_{i,j}$$
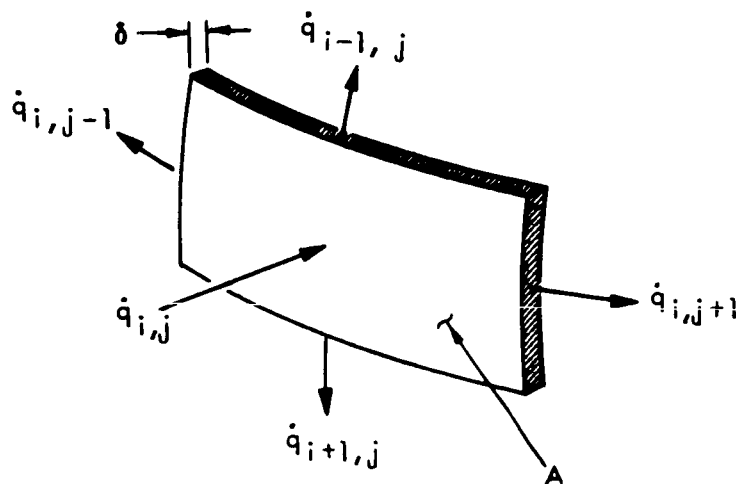
$$V = A\delta$$

$$\rho V C_p \frac{\Delta T_{i,j}}{\Delta\tau} = \Sigma \dot{q}$$

Figure 10. - Single node heat balance.

where

$$\dot{q}_{in} = \dot{q}_a + \dot{q}_s + \dot{q}_R + \dot{q}_E$$

= aerodynamic + solar + reflected + emitted,

and

$$\dot{q}_{rad} = \sigma \epsilon T^4.$$

Heat inputs. - The spacecraft is protected from external heating for the first few minutes by the Agena nose shroud. It was assumed that the entire spacecraft was at 70°F when the nose shroud was ejected. When the spacecraft is exposed, it receives aerodynamic heating, $\dot{q}_a$, direct solar heating, $\dot{q}_s$, reflected solar heating, $\dot{q}_R$, and earth radiated heating, $\dot{q}_E$, as shown in Figure 11.
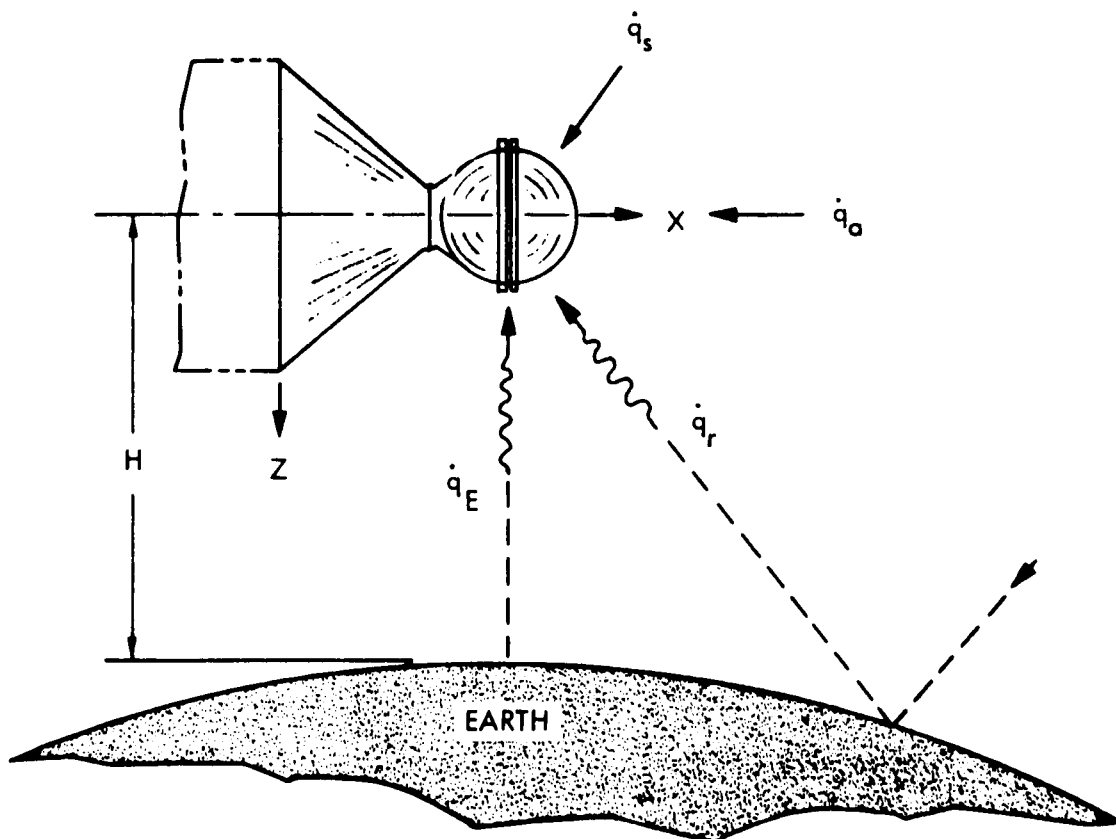
Figure 11. - Heat inputs.

Aerodynamic heating: The aerodynamic heating is significant for approximately ten minutes after shroud ejection. The equation used to determine the aerodynamic heat flux for free molecular heating was:

$$\dot{q} = 1/2 \ W/g \ U^2$$

$$= 1/2 \ (\rho/g \ U \ A) \ U^2$$

$$= 1/2 \ \rho/g \ U^3$$

If the above equation is normalized to sea level density and satellite velocity, the following equations are resolved.

$$\dot{q}_s = 2.65 \times 10^7 \left(\rho_\infty / \rho_0 \right) \left(U_\infty / 26000 \right)^3$$

$$\dot{q}_{fp} = 0.44 \times 10^7 \left(\rho_\infty / \rho_0 \right) \left(U_\infty / 26000 \right)^2 \left(\bar{U} / 26000 \right)$$

$\bar{U}$ = Molecular velocity

$\dot{q}_s$ = Stagnation point heat flux

$\dot{q}_{fp}$ = Flat plate heat flux

Radiative heating: The spacecraft receives radiative heating from the time of shroud separation until the payload is injected into orbit. This consists of (1) direct solar radiation which will be a function of the spacecraft's orientation relative to the solar vector, (2) earth radiation as a function of the spacecraft's orientation relative to the planet vector and the spacecraft's altitude, and (3) earth reflected solar radiation which will be a function of spacecraft's altitude and its orientation relative to both the solar vector and the planet vector. All of these are shown in Figure 12 for a node i, j, having a normal vector at its surface of $\bar{N}_{i,j}$.

Figure 12. - Solar, planet-node vector definition.

After shroud ejection, the X axis is parallel to the earth's horizon so that the planet vector $\bar{P}$ is along the Z axis.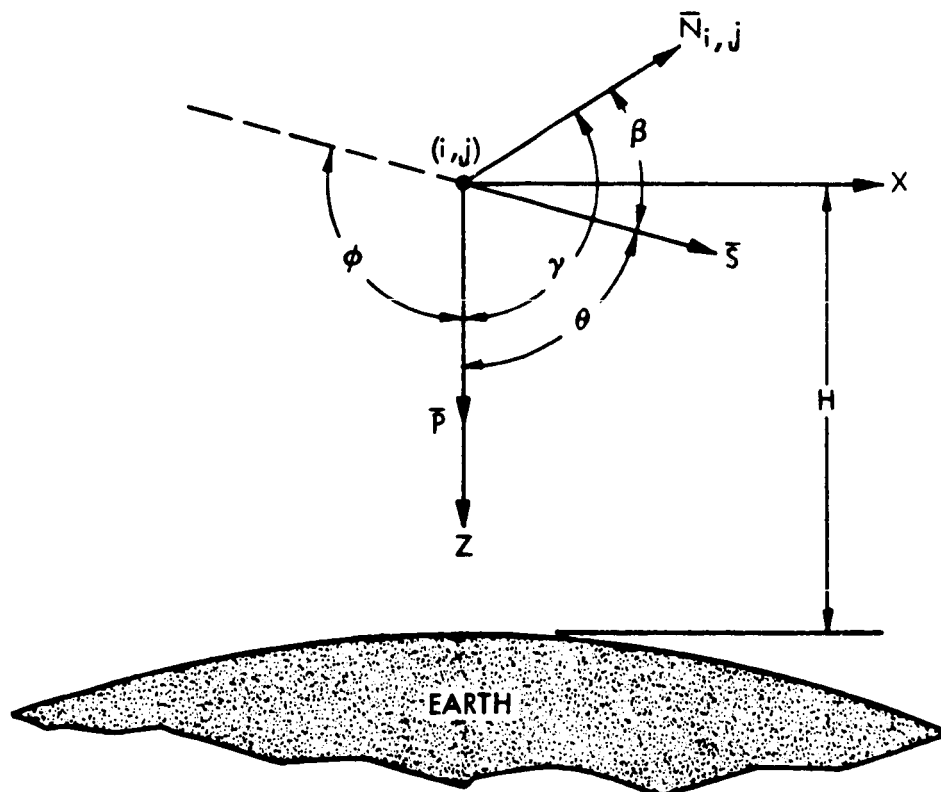 The canister assembly geometry, as shown in Figure 8, was programmed into the shape factor routine of an existing program previously developed at GAC, see Reference 1. The first part of this program calculates the altitude and the direction cosines, $\bar{x}_S$, $\bar{y}_S$ and $\bar{z}_S$, of the solar vector $\bar{S}$. The program then proceeds into the shape factor routine and defines the normal vector $\bar{N}$ for each node in terms of the direction cosines, $\bar{x}_N$, $\bar{y}_N$ and $\bar{z}_N$. The program then calculates the angle between any two vectors such as $\bar{N}_{i,j}$ and $\bar{S}$, by taking the scalar product

$$\beta_{i,j} = \text{Cos}^{-1} (\bar{x}_N \cdot \bar{x}_S + \bar{y}_N \cdot \bar{y}_S + \bar{z}_N \cdot \bar{z}_S) ,$$

which is then used in the view factor routine and the heat flux routine to obtain the heat fluxes described in the following sections. Optical properties of the surfaces are not included here so that the output from this program is the incident heat fluxes.

(1) For direct solar radiation a solar constant, C_S, of 443 Btu/Hr-Ft^2, was assumed incident on the spacecraft, except when it was in the umbra. The spacecraft is in the umbra when

$$\text{Sin } \theta \; < \; \frac{RP}{RP + H}$$

and

$$\text{Cos } \theta \; > \; 0.$$

For any node, the direct solar heat flux, $\dot{q}_S$, is a function of the projected area A_p.

$$\dot{q}_S = C_S A_p ,$$
$$= C_S A \text{ Cos } \beta .$$

if

$$\text{Cos } \beta \; \leq \; 0,$$

$$\dot{q}_S = 0.$$

(2) The earth was assumed to be an isothermal sphere radiating diffusely. The intensity of the heat flux at the surface of the earth E_O, was obtained by taking the amount of solar energy absorbed by the projected area and distributed over the entire spherical area.

$$E_O = (1 - a) C_S \left(\frac{\pi \, RP^2}{4\pi \, RP^2} \right) ,$$
$$= \frac{1 - a}{4} C_S .$$

At any altitude H, the heat flux, E, incident on a flat plate parallel to and facing the earth surface is proportional to the inverse square law.

$$E = E_o \left(\frac{RP}{RP + H} \right)^2 .$$

For the general case, where the surface normal, $\overline{N}$, can be pointing in any direction, a different method of calculating the heat flux is necessary.

The point source method was selected. These view factors were developed in Reference 2.

(3) The earth was assumed to have an albedo of 0.4 and to be reflecting diffusely. The incident heat flux on any node of the spacecraft used the same view factors FP's, as were used for earth radiation. The heat flux intensity in this case differs from the earth radiation heat flux because it is not constant. At the earth's surface, the intensity is a maximum on the earth sun-line and is assumed to decrease as the cosine of the angle between the earth-sun line and the earth-satellite line. This angle is $\emptyset$. As the satellite altitude increases, the intensity at the maximum point, which is the earth-sunline, decreases. However, for the angle of $\emptyset$ equal to or greater than 90°, the intensity increases with satellite altitude since the satellite can begin to see part of the reflecting spherical area. Equations for this distribution and intensity were developed in Reference 2. An empirical equation was included in GAC's heat flux program. This gives a curve fit for the first 1,000 miles. Since the flux is low at the $\emptyset = 90°$ point, for altitudes above 1,000 miles the absolute value of the heat flux is so small that the empirical equation was considered a satisfactory fit.

Analysis. - The heat transfer equations were written to include the heat inputs described in the previous subsection, along with the heat capacity and thermal resistors of the nodes to enable calculation of the temperatures as a function of time. The basic three dimensional transient heating equation is

$$\frac{dT}{d\mathcal{T}} = \alpha' \nabla^2 T + \frac{\dot{q}}{\rho C_p}$$

Rewriting this in finite difference form results in

$$(\Delta x \, \Delta y \, \Delta z) \frac{\Delta T_{x,y,z}}{\Delta \mathcal{T}} = \alpha' \left[\frac{T_{x-1,y,z} + T_{x+1,y,z} - 2T_{x,y,z}}{\Delta x} \right.$$

$$+ \frac{T_{x,y-1,z} + T_{x,y+1,z} - 2T_{x,y,z}}{\Delta y} + \left. \frac{T_{x,y,z-1} + T_{x,y,z+1} - 2T_{x,y,z}}{\Delta z} \right]$$

$$+ \frac{\dot{q} - A \sigma \epsilon T^4_{x,y,z}}{\rho C_p}$$

Since the spacecraft structure is assumed to be thermally thin, the finite difference equation used has two dimensions, i and j, resulting in

$$c \delta A \, \frac{\Delta T_{i,j}}{\Delta T} = \frac{T_{i-1,j} - T_{i,j}}{RL_i} + \frac{T_{i+1,j} - T_{i,j}}{RL_{i+1}} + \frac{T_{i,j-1} + T_{i,j+1} - 2T_{i,j}}{RC_i}$$

$$+ \dot{q} - \sigma \epsilon A \, T^4_{i,j}.$$

Spacecraft: To perform the thermal analysis, a starting point of defining a launch window is required. This, along with the ascent trajectory is used to generate a heat flux tape. The physical dimensions and properties of the spacecraft are used to generate a matrix inversion tape. These tapes are then used over and over again with any number of different thermal control patterns.

Flight launch window: A number of launch windows were defined for a period from 1 June 1966 to 1 September 1966. These were given in terms of initial orbit right ascensions. For a selected launch window, both the opening and closing times were used along with the ascent trajectory to determine the heat fluxes and the thermal control coatings required.

The coatings selected were evaluated for the trajectory extremes referred to as three sigma high and three sigma low. The original pattern, which was designed for a 21 June 1966 launch, would satisfy the temperature control requirements until 15 July. A launch occurring after 15 July required an additional or modified pattern of the original coating. A pattern was determined to maintain safe temperatures for a 15 July to 4 August launch period and was designated as the "second pattern." Table I shows the tape patterns for the "original" and "second" coatings as percentage of aluminum tape on a white enamel surface.

Prototype launch window: The prototype canister assembly was tested in a space chamber to check the validity of the analytical thermal model. The heat flux tape was generated for a 21 June, 87.5° inclination prograde orbit having a right ascension of 360° or 0°, with no free molecular heating. This simplified heating simulation was chosen because three things would have been difficult to simulate: (1) a variable earth radiation, (2) free molecular heating and (3) moving radiant heat inputs. The free molecular heating would have been most difficult; the variable earth radiation (both intensity and viewing angle) would have been the second most difficult; and the moving heat flux, such as the solar vector, would have been the least difficult, but even it would have required that the canister assembly and the infrared banks be mounted on a moveable platform.

Results. - The results presented here are for both the prototype and the spacecraft.

Prototype: The thermocouple that reached the maximum and minimum temperatures for both the canister assembly and the adapter are shown in Figure 13. Also shown are the calculated time-temperatures of the area represented by the thermocouple. With the exception of one area on the adapter, all of the test temperatures were lower than predicted. The area on the adapter that read higher than the calculated temperatures was probably due to the result of
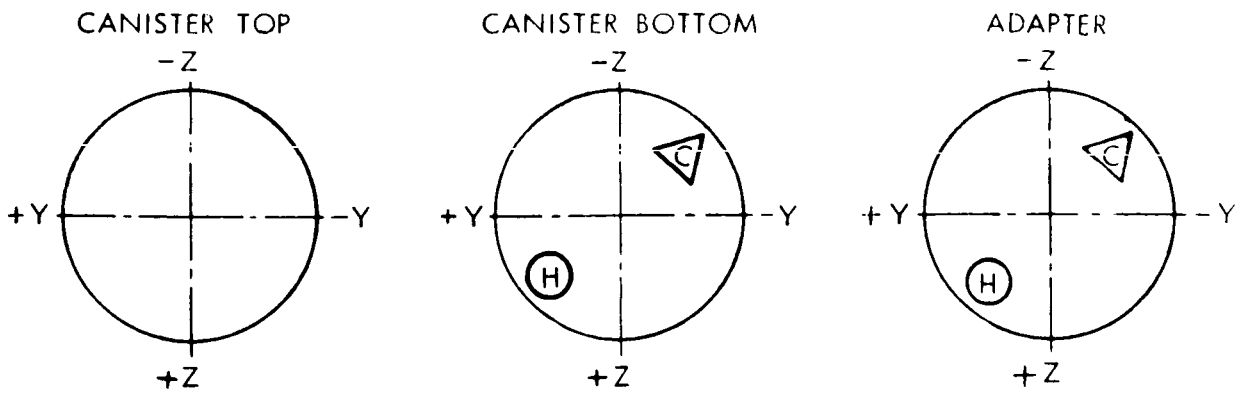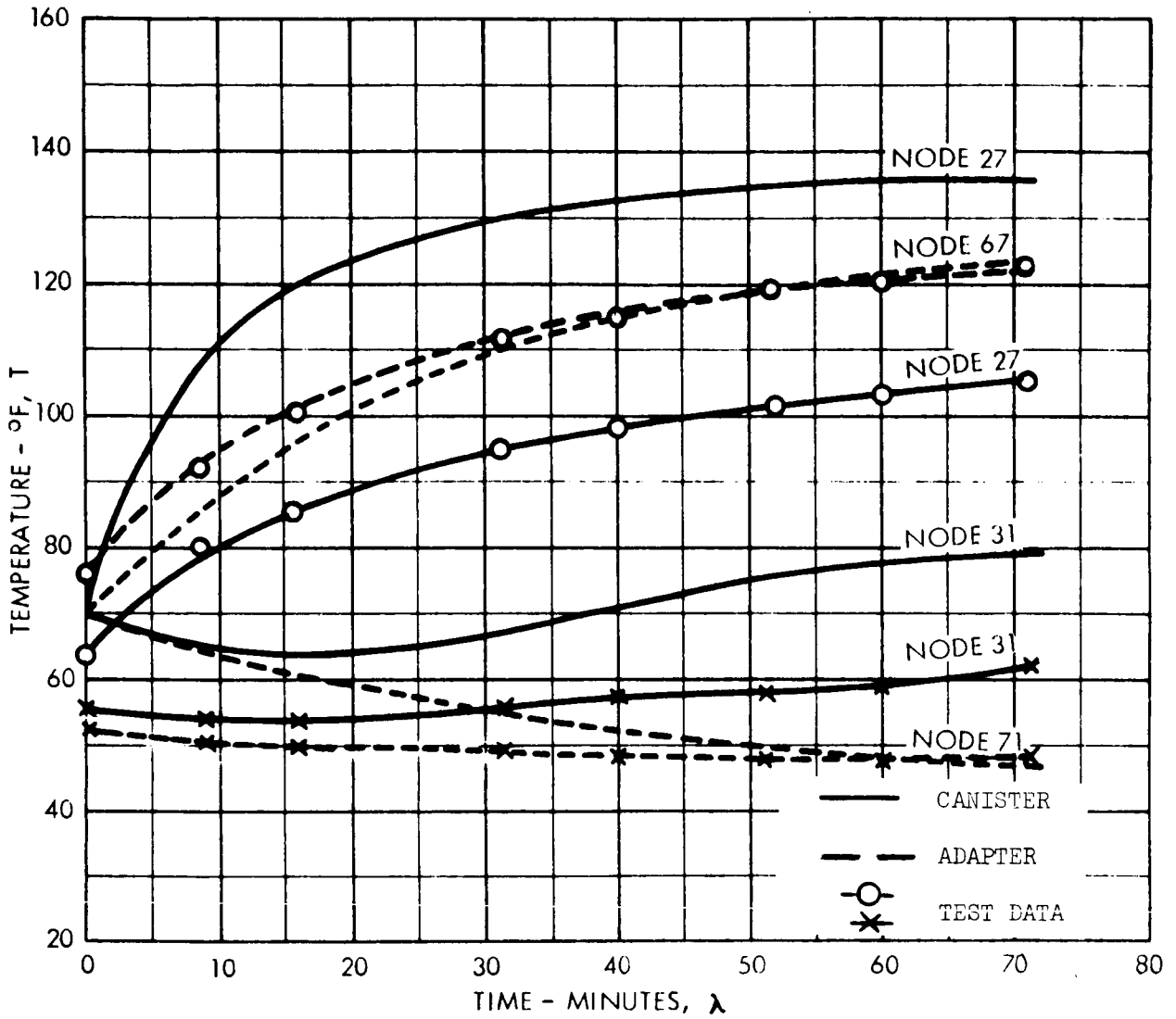
Figure 13. - Time-temperature of prototype.

adjusting (tilting one row of lights toward the adapter) the infrared heating to compensate for the large adapter size. The major portion of the canister assembly reading cool was probably the result of the heat flux decreasing with the distance from the reference plane which was set at the close edge of the canister. It was not possible to maintain the assembly at 70°F during the few hours of cool down of the space chamber walls, but the 10 or 15°F variation should have been greatly reduced during the 72 minutes heating cycle since most temperatures begin to come in asymptotically to an equilibrium condition. The general thermal response and distribution compare well enough to verify the validity of the analytical thermal model. The prototype pattern is shown in Table I.

Flight temperature-time histories: The analysis conducted was obtained for the following launch conditions and thermal patterns:

Original flight pattern (21 June through 14 July)

Nominal trajectory	Right ascension (Degrees)
(1) 21 June window opening	351.5
(2) 21 June window closing	346.5
(3) 14 July window opening	351.0
(4) 14 July window closing	6.0

3 Sigma high trajectory	
(1) 21 June window opening	351.5
(2) 21 June window closing	346.5
(3) 14 July window opening	351.0
(4) 14 July window closing	6.0

3 Sigma low trajectory	
(1) 21 June window opening	351.5
(2) 21 June window closing	346.5
(3) 14 July window opening	351.0
(4) 14 July window closing	6.0

Second flight pattern (15 July through 4 August)

Nominal trajectory	
(1) 15 July window opening	56.0
(2) 15 July window closing	71.0
(3) 4 August window opening	78.5
(4) 4 August window closing	93.5

3 Sigma high trajectory	
(1) 15 July window closing	71.0
(2) 4 August window closing	93.5

3 Sigma low trajectory	
(1) 15 July window opening	56.0
(2) 4 August window opening	78.5

TABLE I

TAPE PATTERNS

Node	Percentage									
(Prototype patterns)										
1-10	100	90	95	100	100	100	100	100	95	95
11-20	85	100	100	100	100	100	85	60	75	100
21-30	100	100	100	100	75	60	75	100	100	100
31-40	100	100	75	60	75	100	100	100	100	100
41-50	75	70	80	100	100	100	100	100	80	80
51-60	90	100	100	100	100	100	90	80	90	100
61-70	100	100	100	100	90	80	90	100	100	100
71-73	100	100	90	--	--	--	--	--	--	--
(Original patterns)										
1-10	70	70	70	70	70	80	85	85	75	50
11-20	70	100	100	100	100	100	75	50	40	100
21-30	100	100	100	100	75	50	70	80	100	100
31-40	100	100	90	55	55	80	100	100	100	100
41-50	75	50	50	90	100	100	100	100	85	70
51-60	65	75	100	100	100	100	75	75	75	75
61-70	100	100	100	100	90	75	75	75	100	100
71-73	100	100	100	--	--	--	--	--	--	--
(Second patterns)										
1-10	70	70	70	70	70	80	85	85	75	70
11-20	70	100	100	100	100	100	75	70	60	100
21-30	100	100	100	100	75	90	90	100	100	100
31-40	100	100	90	95	100	100	100	100	100	100
41-50	100	100	100	100	100	100	100	100	100	85
51-60	80	80	100	100	100	95	80	80	80	80
61-70	100	100	100	90	80	75	80	80	100	100
71-73	100	90	80	--	--	--	--	--	--	--

Figures 14 and 15 show typical plots of the hottest and coldest nodes as a function of time for the three sigma high, nominal and three sigma low trajectories for a 21 June launch, for a window opening and closing condition. The above temperatures are for the canister only.
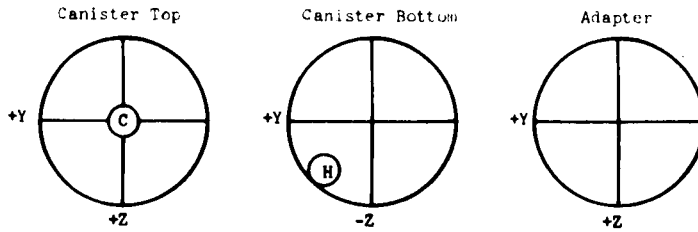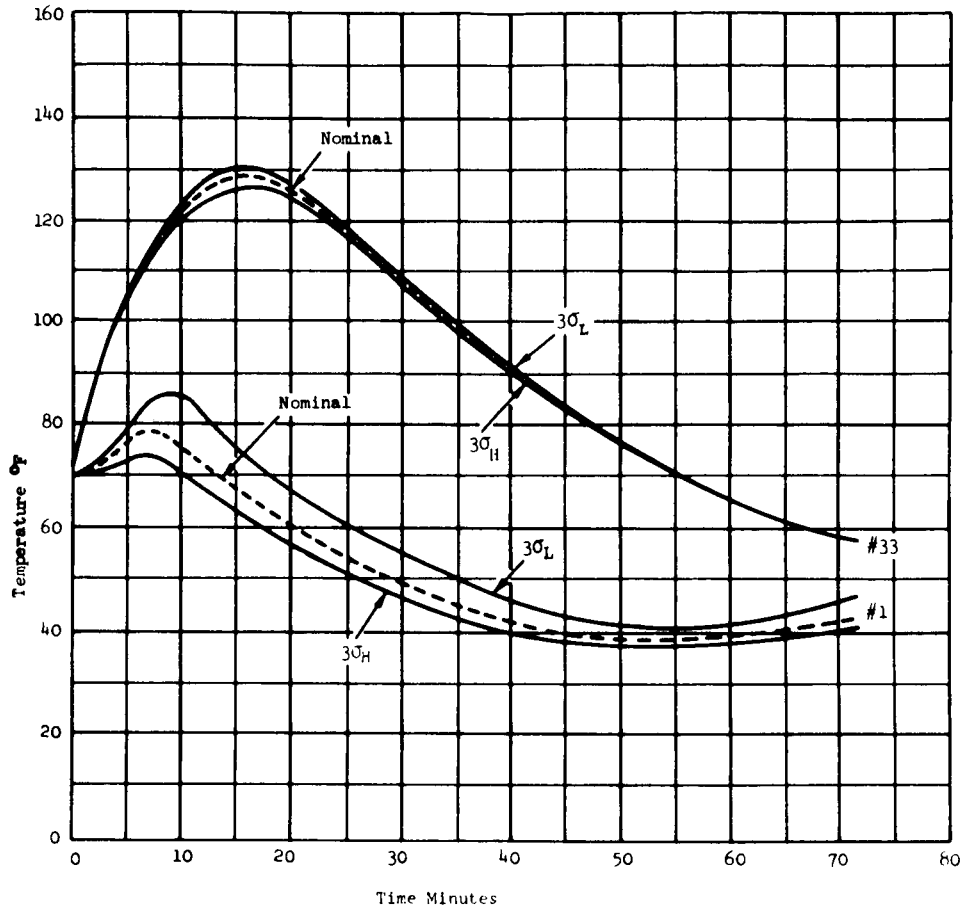
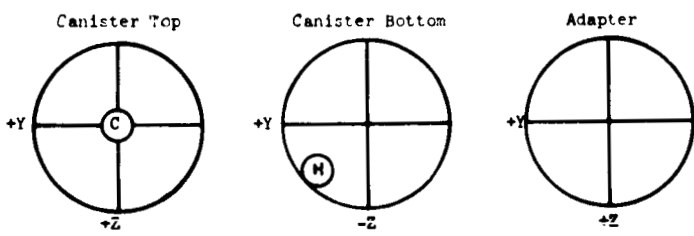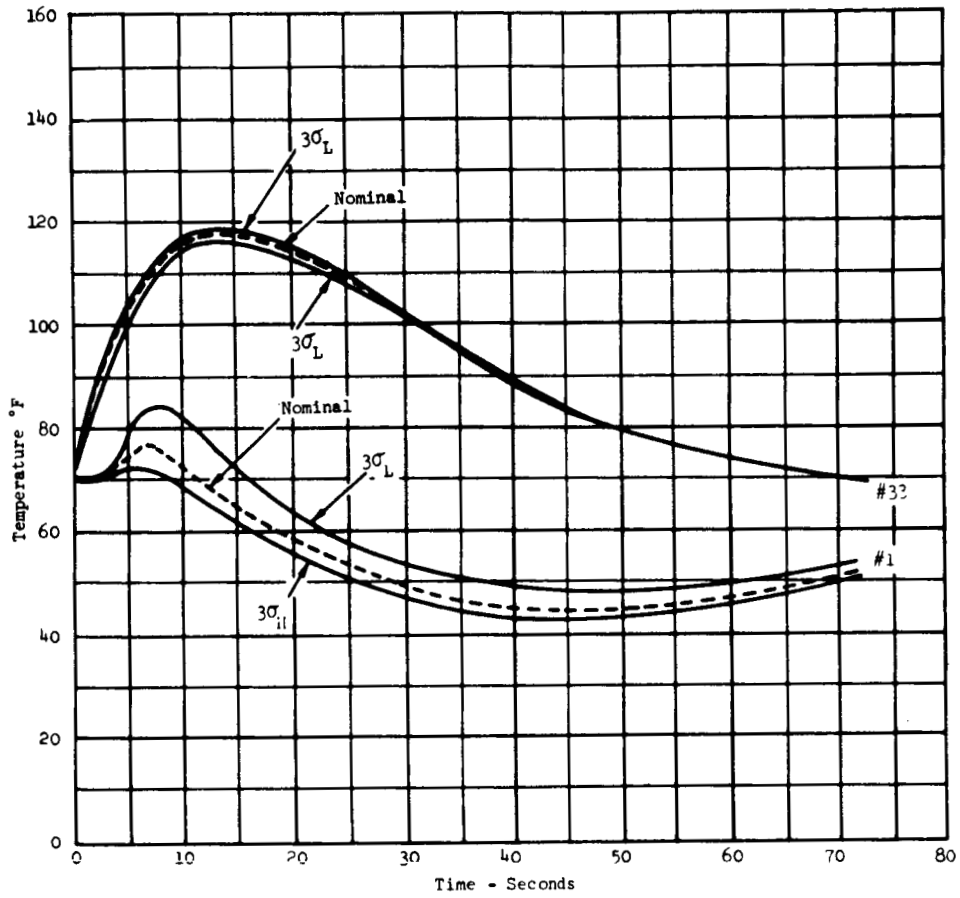Figure 14. Canister temperature for window opening, 21 June

Figure 15. Canister temperature for window closing, 21 June

Conclusions. - It was concluded, from the thermal analysis that the canister assembly would remain between the desired temperature limits of (32°F to 140°F) for the flight duration of shroud-off to satellite ejection. The temperature of the adapter assembly, however, was predicted to extend above and below these limits by approximately 15° during this period. These temperature extremes occur at the aft end of the assembly and play no part in the success of the mission as no temperature sensitive components are located in this area.

Structural Analysis

Description. - The canister, as shown in Figure 3, consists of an upper and lower canister half constructed of ZK60A-T5 magnesium die forgings. The canister is spherical in shape with an inside radius of 13.25 inches. The equatorial rings are an integral part of the two halves with a gradual transition to the basic shells. The rings are machined to accept holes for valves and transducers, and hoisting lugs. Various components such as batteries, timers, etc., are located at the bottom of the lower canister half.

The adapter is a frustum of a cone utilizing riveted aluminum alloy sheet-stringer construction, 25.3 inches high tapering from a diameter of 60 inches at the base to 11.8 inches diameter at the top. Transverse stiffening consists of the upper plate and lower and intermediate rings. Longitudinal stiffening consists of eight primary and eight intermediate angles. Attachment to the Agena vehicle is made through eight attachment bolts and to the canister by a quick-release clamp. Two of the primary stiffeners support the instrument box.

The principal structural components of the ejection system for separating the canister from the adapter are a single ejection spring and a quick-release clamp.

Design constraints. - Many of the constraints that affected the structural design of the canister assembly, which can not be conveniently presented in the normal presentation of the analysis, are discussed below in the following paragraphs.

Lower canister thickness: The minimum thinkness (0.060 inch) is the same as that used on the Echo I canister. This selection was made on the assumption that the buckling strength of the Echo I canister was satisfactory.

Upper canister thickness: The shell thickness is dictated by the desire to keep the upper and lower canister half approximately equal in weight. It is thicker than required for structural reasons.

Equatorial rings: The geometry of the equatorial rings on the canister halves was selected on the basis of engineering judgment considering Echo I and Echo II ring designs in conjunction with the PAGEOS requirements. The substantiation of the chosen design was by test.

Natural frequency of the spacecraft: A considerable portion of the design was dictated by the desire to have the lowest natural frequency considerably higher than the POGO frequency (17-22 cps) rather than strength.

Damping: In order to provide as much damping as possible, a rivited construction was used for the adapter.

Aerospace ground equipment: The canister assembly and AGE design were an integrated effort to provide all of the pre-launch handling capabilities required with a minimum weight and reliability penalty to the canister assembly itself.

Design criteria. - The design limit load conditions were selected from consideration of design criteria and the qualification test program. In addition, load combinations that might result in critical in-flight loading are included based on spacecraft external pressure and acceleration versus flight time data presented in Figure 16.

Dynamic amplification factors for the various load conditions are chosen on a best estimate basis.

All dynamic load calculations assume that the balloon is infinitely rigid and responds 1 to 1 to all canister motions.

Dynamic amplification factors. - The three factors considered are:

Amplification factors for sinusoidal excitations: C/C_c of a damped single-degree-of-freedom system that ranges from 0.01 to 0.04 (Reference 3, page 87) will have dynamic amplification factors ranging from 50 to 12.5 respectively when subjected to sinusoidal excitations. This range of C/C_c is typical for a riveted type of aircraft structure, such as the PAGEOS adapter. However, PAGEOS obtained additional friction damping from the canister separation clamp. The maximum amplification factor from testing an old Echo I canister was 5.7. Based on the above information, a dynamic amplification factor of 10 was chosen as representative of the PAGEOS dynamic response to sinusoidal excitation along any axis.

Amplification factor for longitudinal shock load: A 15 g, 6 to 10 millisecond, half sine wave shock load along the longitudinal axis of the spacecraft was required. Reference 4, page 163, gives the dynamic response of a single degree of freedom system to a half sine wave pulse in terms of the system's period, T, and the pulse width, τ The first mode longitudinal natural frequency of the PAGEOS is calculated to be 153 cps. The dynamic amplification factor for

$$\frac{\tau}{T} = \frac{0.006}{1/153} = 0.92$$

is equal to 1.8.

Accelerations due to random vibrations: Random vibration of the PAGEOS spacecraft resulted in the following canister accelerations:
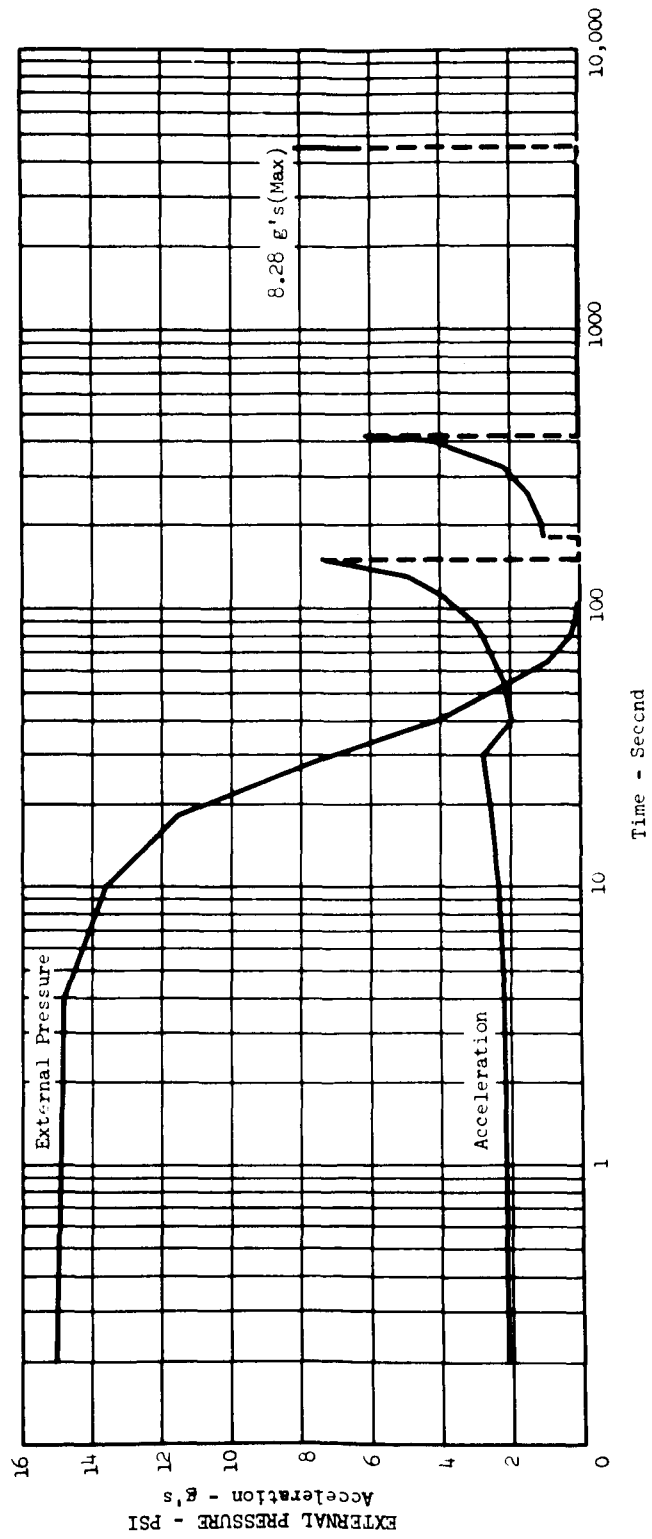
Figure 16. - Pressure and accelerations versus time.

8.28 g's (Max)

External Pressure

Acceleration

Time - Second

EXTERNAL PRESSURE - PSI
Acceleration - g's

38

(1) Transverse and normal acceleration:

The PAGEOS transverse and normal first pitching mode natural frequency is calculated to be 38.7 cps. Assuming the power spectral density curve in this frequency range is white noise with $G_0 = 0.005$ g^2/cps and that the sinusoidal amplification factor, θ, is 10; the rms acceleration is given as

$$A_r = \sqrt{\frac{\pi}{2} G_0 f_0 \theta} = \sqrt{\frac{\pi}{2} \times 0.005 \times 38.7 \times 10} = 1.74 \text{ rms g}$$

The peak acceleration is

$$A_r = 1.74 \times 1.41 \approx 2.5 \text{ g}$$

(2) Longitudinal acceleration:

The longitudinal first mode natural frequency is calculated to be 153 cps. With the same assumptions regarding white noise and sinusoidal amplification factors, the rms longitudinal acceleration due to random vibration is given as

$$A_r = \sqrt{\frac{\pi}{2} G_0 f_0 \theta} = \sqrt{\frac{\pi}{2} \times 0.005 \times 153 \times 10} = 3.43 \text{ rms g}$$

The peak acceleration is

$$A_r = 3.43 \times 1.41 \approx 5g$$

Load conditions. - The following design limit load conditions were established for the design of the PAGEOS canister assembly.

It is convenient to denote the evacuated canister assembly as a basic condition. "Basic" is the condition of 14.7 psi external pressure differential plus the ejection spring load of 500 lbs.

Condition A. Basic + 11 g's axial.

Condition B. Basic + 2.5 g's transverse.

Condition C. Basic + 15 x 1.8 = Basic + 27 g's axial.

Condition D. Basic + 3 x 10 = Basic + 30 g's axial.

Condition E. Basic + 1 x 10 = Basic + 10 g's transverse.

Condition F. The canister ejection velocity - six feet per second, minimum.

Condition G. The canister opening system shall impart a minimum velocity of 20 feet per second to each half of the canister, relative to the opening plane, when operating in a vacuum of 10^{-2} torr or lower pressure. The equatorial flange and canister half shall not crack, break, or be seriously damaged by the canister opening.

Condition H.   Basic + 2.5 g's transverse + 8 g's axial.
This combined condition is a low altitude flight
condition. It considers the nominal flight trajectory
shown in Figure 16 in which a steady state axial
acceleration of 3 g's combines with the external
pressure and spring load plus an estimated 2.5 g's
transverse plus 5 g's axial based on random vibration
qualification test levels.

Condition J.   Ejection spring load + 10 g's transverse + 15 g's
axial. This combined condition is a high altitude
flight condition. It considers the nominal flight
trajectory shown on Figure 16 in which a high axial
acceleration is attained when the pressure differ-
ential is essentially zero. The combination of
transverse and axial loads cover the base where large
axial accelerations may be combined with the maximum
transverse vibrational acceleration.

Condition K.   Hoisting. A load factor of 5 shall be used for hoisting
in a vertical position.

Condition L.   Working. A load factor of 2 shall be used for working
on the canister in the horizontal position.

Allowables.   The sources for allowable stresses and loads are:

(1)   Strength of aircraft elements.

(2)   Contractor's structural manual.

(3)   Standard references.

(4)   Tests.

Factors of safety. - The factors of safety for the canister assembly
are 1.00 for yield and 1.5 for ultimate.

The minimum margin of safety determined by this structural analysis
are shown in Table II.

Vibration test results.   During the design phase of PAGEOS the
natural frequencies were calculated as a coupled mode system. The calculation
procedure utilized matrix methods and influence coefficients. Two separate
analyses were conducted. One analysis assumed that the packaged sphere
(which weighs 149.25 pounds) was infinitely rigid and moved with the
canister (which weighs 39.28 pounds) as if the two component parts were
one solid mass weighing 188.53 pounds. The calculated natural frequen-
cies for the 3 normal modes utilizing this assumption are as follows:
f_1 = 37.9 cps (pitching about a point at the bottom of the canister),
f_2 = 153 cps (plunging along X axis), and f_3 = 183 cps (pitching about
a point at top of canister).

TABLE II

MINIMUM MARGINS OF SAFETY

Item	Critical Condition	Critical Stress	M.S.
Canister			
Top Shell	D	Buckling	High
Bottom Shell	Basic,B,E	Compression	0.28
Lacing	Rebound	Tension	0.81
Adapter			
Stringer	J	Buckling	0.43
Skin	J	Shear	0.36
Bottom Ring	J	Tension	5.17
Top Ring	J Clamp	Compression	1.38
Rivet	J	Shear	0.11
Attachment Bolt	Preload	Tension	0.94
Clamp			
Explosive Bolt	Preload	Tension	0.00
Band	Preload	Tension	0.05
Block	Preload	Bending	1.80
Ejection Spring	Installation	Shear	0.02

The 3 values for natural frequency were also calculated assuming that only the canister weight determined the natural frequency, since it was assumed that the sphere is so flexible and heavy that inertia effects would prevent the sphere from following the canister. In other words, the weight of the packaged inflatable sphere would be vibration isolated from the canister walls. The values of the 3 normal modes calculated using this assumption are as follows: $f_1 = 85$ cps, $f_2 = 342$ cps, and $f_3 = 410$ cps.

The values determined by test showed that the first assumption was correct since the measured natural frequency was 37 cps compared to the 37.9 cps calculated. The damping due to the packaged envelope and the quick release clamps at the canister/adapter separation joint was so great $(C/C_c = 30\%)$ resulting in an amplification factor equal to 1.7 that it was extremely difficult to find this lowest natural frequency from the tape recorded output. It could only be found from the sinusoidal sweeps since the acceleration value of the response was too small to detect during the random sweeps. The RMS acceleration is proportional to the square root of the amplification factor or the RMS acceleration is proportional to $\sqrt{Q}$.

For the two higher frequency normal modes, the tape recorded responses were very clear and consistent. The measured values of response showed $f_2 = 205$ cps, and $f_3 = 240$ cps. The significance of these values is that only a portion of the inflatable packaged envelope (47%) moved with the canister. The other 53% remained stationary in space as if vibration isolated.

To determine the percent of envelope that participated in determining the measured natural frequency, the following simplified analysis was used:

For each normal mode $f_i = 3.13 \dfrac{K_i}{W_i}$ where K is the spring constant in pounds per inch and "W" is the weight of canister (39.28 lb) plus weight of packaged envelope that moves with the canister. The value for "K" was calculated and verified by static test so was quite reliable. From the knowledge of K and the measured natural frequency, it was possible to calculate W. From this value of W the canister weight of 39.28 pounds was subtracted resulting in the weight of the envelope which participated in determing the measured natural frequencies. The weight divided by the total envelope weight determined the 47% number previously stated. The same percentage 47% was calculated both for the plunging mode f_2 = 205 cps and the second pitching mode f_3 = 240 cps.

Weights

A weight breakdown for the prototype, Canister Assemblies No. 3, No. 4 and No. 5 are shown in Table III. The calculated and actual (for Canister Assembly No. 4) center of gravity and moment of inertia is shown in Table IV.

TABLE III
CANISTER ASSEMBLY WEIGHTS

Item	Proto-type	Canister Assembly No.		
		3	4	5
Canister - Upper Half		17.20	17.25	17.65
Thermal Tape		+0.59	+0.59	+0.59
Cover - Solenoid Valve		+0.07	+0.07	+0.07
Cover - Terminal Board		+0.03	+0.03	---
Total Actual Weight - Upper Half	17.78	17.89	17.94	18.31
Canister - Lower Half		18.90	18.75	19.40
Thermal Tape		+0.39	+0.39	+0.39
Cover - Protective		+0.02	+0.02	+0.02
Cover - Protective		+0.03	+0.03	+0.03
Battery Pack		+1.69	+1.69	+1.69
Battery Pack Hardware		+0.03	+0.03	+0.03
Arming Plug		+0.06	+0.06	+0.06
Total Actual Weight - Lower Half	20.99	21.12	20.97	21.62
Opening System	0.51	0.51	0.51	0.51
Total Canister	39.28	39.52	39.42	40.44
Adapter		50.25	50.18	50.40
Thermal Tape		+0.90	+0.90	+0.90
Interface Bolts and Washers		+0.30	+0.30	+0.30
Cables - Clamp Band & Hardware		---	+0.22	---
Eye Bolts For Cables (6)		---	---	+0.06
Total Actual Weight - Adapter	51.14	51.45	51.60	51.66
Total Canister Assembly (Lbs.)	90.42	90.97	91.02	92.10

TABLE IV

PAGEOS SPACECRAFT MASS PROPERTIES

Mass Parameters	Launch Condition		Orbit Condition[a]	
	1[b]	2[c]	1[b]	2[c]
Weight (lbs.)	255.4	240.27	51.14	51.60
C.G. Location X (inch from interface)	35.27	43.93	13.54	13.54
Y (inch from centerline)	-0.11	-0.26	-0.57	-0.57
Z (inch from centerline)	-0.24	-0.11	-1.19	-1.19
Moment of Inertia I_X (slug ft.^{2})	7.43	7.23	3.86	3.89
I_Y (slug ft.^{2})	12.86	12.57	2.79	2.82
I_Z (slug ft.^{2})	12.89	12.60	2.87	2.90
Product of Inertia I_{XY} (slug ft.^{2})	0.11	0.10	-0.03	0.03
I_{XZ} (slug ft.^{2})	0.30	0.30	0.02	0.02
I_{YZ} (slug ft.^{2})	0.05	0.05	0.04	0.04
Satellite (Lbs.)	----	----	165.0	149.25

a. Adapter only
b. Calculated
c. Actual for Spacecraft No. 4

TEST PROGRAM

General

The PAGEOS test program was divided into three major test phases, i.e., Development Tests, Qualification Tests and Flight Acceptance Tests. In general, the objectives of each test phase were as follows:

(1) Development Program - To verify the initial canister design adequacy through tests of components, materials and subsystems.

(2) Qualification Program - To verify the final canister assembly design, including inflatable sphere, under extreme environmental and operational conditions.

(3) Flight Acceptance Program - To verify the quality of materials and workmanship employed in the construction of the canister assemblies.

Development Test Program

The specific objectives of the Development Test Program were as follows.:

(1) To verify the general design and performance of the canister opening and ejection system.

(2) To ensure that all materials and components utilized in the fabrication of the flight unit were adequate for the environment they would experience during the mission.

(3) To determine the structural adequacy of the canister and to verify the adequacy of the canister seals.

The tests, which were performed to meet these objectives are as follows:

Canister Ring Separation Test No. 1

Canister Ring Separation Test No. 2

Canister Ring Separation Test No. 3

Canister Ring Separation Test No. 4

Evacuation and Leak Rate Test

Implosion Test

Canister Ejection Test

Materials Test

Canister Ring Separation Test No. 5

Canister Ring Separation Test No. 6

Component Tests

Canister Ring Separation Test No. 7

Canister Ring Separation Test No. 8

Ring separation tests. - The ring separation tests consisted of firing the flexible linear shaped charge in dummy ring sections to simulate each canister half. The following results were required during three tests in air and one in vacuum:

(1) To achieve a separation velocity of 20 ft/sec. with each ring.

(2) To verify structural integrity of the canister flanges.

In all, eight tests were required before the desired final results were achieved. Three initial tests were performed with nominal 30 grain/ft shaped charge. One 40 grain/ft charge was fired to verify flange design. After low velocities were obtained in the vacuum test, the nominal grain size was raised to 40 grain/ft. To prove the flange design, a 50 grain/ft (nominal) charge was fired. Mean velocities for all 40 grain/ft tests were 30.30 ft/sec (upper half) and 27.49 ft/sec (lower half).

Evacuation and leak rate tests. - Evacuation tests were performed to ensure that the canister structural integrity was adequate to withstand static loads simulating peak mission environments for vibration and acceleration. In addition, the canister was required to demonstrate a maximum leak rate of 0.10 torr over a 24-hour period. Initially, Canister No. 1 was evacuated to approximately 0.85 torr. The leak rate test was then completed after 36 hours with a leak rate of 0.08 torr over the final 24-hour period. Static loads were then applied and it was determined that at no time did elastic deformation approach the yield value of the canister material. From the results of strain gage data, it was concluded that no permanent set of the structure had occurred.

Implosion test. - The implosion test was conducted to determine critical buckling pressure of the Canister No. 1. Differential pressure was applied to the canister (positive on external side) using a hydroclave. Differential pressures of 50 psi and 100 psi were applied on two subsequent runs. From this test, it was concluded that buckling of the lower canister started at a differential of 80 psi and that the canister would sustain maximum differential pressure of 102 psi. The structural integrity of the canister was concluded to be adequate.

Canister ejection test. - The canister ejection test was performed to determine the relative separation velocity between canister and adapter obtained with the ejection spring. The test was performed using the Canister No. 1 and a dummy weight to simulate an expended Agena motor. Two tests were conducted to ensure that the minimum separation velocity of 6 ft/sec was reached when either both or only one of the clamp separator explosive bolts were fired. Both tests were performed with the full assembly in horizontal free fall, and the following velocities were obtained:

(1) Test No. 1 (both explosive bolts) velocity was 8.12 ft/sec.

(2) Test No. 2 (one explosive bolt) velocity was 7.79 ft/sec.

It was concluded from the above results that the canister ejection system was adequate. No damage to the canister or adapter was sustained.

Material tests. The tests of 13 materials consisted of the necessary exposure to mechanical loading, high vacuum, and temperature to verify that no loss of performance would occur which could be detrimental to the successful completion of the mission. The results of these tests were considered satisfactory and showed no unexpected values.

Component tests. - Components for the canister assembly were tested
in two phases:

(1) Performance tests

(2) Environmental tests

Each component had been subject to specified levels of:

(1) Vibration (3 axis - sinusoidal)

(2) Temperature

(3) Acceleration

(4) Shock

(5) Altitude

The tests were conducted to determine that mission environments would not
have a detrimental effect on the functional operation of each component
as installed in a simulated flight configuration. The performance tests
were initially conducted to determine that specified performance tolerances
for individual components were met. During and after subsequent environ-
mental tests, component functions were again checked to determine that
operation remained within specified tolerances. From the results of the
tests discussed above, it was determined that the components selected for
use would operate within the environmental conditions listed below:

Temperature Test

LOW TEMP	Store for 1 hour at 0° F. Raise temperature to 10° F before energizing equipment.
HIGH TEMP	Store for 1 hour at 170° F. Lower temperature to 160° F before energizing equipment. NOTE: For the DC-AC Converter, storage and operating temperatures were 140° F.

Vibration Test (Sinusoidal)

FREQUENCY	10 to 27 cps	27 to 2000 cps
LEVEL	0.4 inch D.A.	15 g's
SWEEP	3 sweeps at 1 octave per minute	
DIRECTION	3 orthogonal axes, relative to the vehicle thrust axis	

Acceleration Test

11 G's Steady State for 7 minutes in the thrust axis, 2.5 G's for 2.5 minutes in the other two orthogonal axes.

Shock Test

30 G's; Half-Sine Wave; 6 to 12 millisecond duration in the thrust axis.

Altitude Test (Vacuum)

Store for 90 minutes at 5×10^{-5} Torr before energizing equipment.

NOTE: Functional tests were performed at the beginning and and at the completion of each environmental test.

Qualification Test Program

The objectives of the Qualification Test Program were as follows:

(1) To verify the adequacy of the prototype canister assembly and the prototype sphere to withstand environments in excess of those expected during the launch and trajectory to orbit.

(2) To prove the integrity of the canister seal, separation joint, opening system and inflatable sphere deployment rate on the final canister design configuration.

The tests which were performed to meet these objectives are as follows:

Qualification Acceleration Test
(Simulated Sphere)

Qualification Vibration Test
(Simulated Sphere)

Qualification Shock Test
(Simulated Sphere)

Qualification Noise Test
(Simulated Sphere)

Qualification Thermal Test
(Simulated Sphere)

Prototype Canister Thermal
Systems Test

Qualification Vibration Test
(Prototype Sphere)

Qualification Vacuum Deployment
Test (Prototype Sphere)

Environmental & RF Susceptibility
Qualification Tests of DM25N4
Dimple Motors

Acceleration tests. - The canister assembly, with simulated sphere installed, was qualification tested in the required acceleration environment (see Figure 17 and Table V). The purpose of the test was to assure that the canister assembly and associated systems provided an adequate margin of safety (Table VI) when exposed to the specified acceleration environment in three axes.

During the tests, power was applied to the flight instrumentation system. The following functions were monitored for performance:
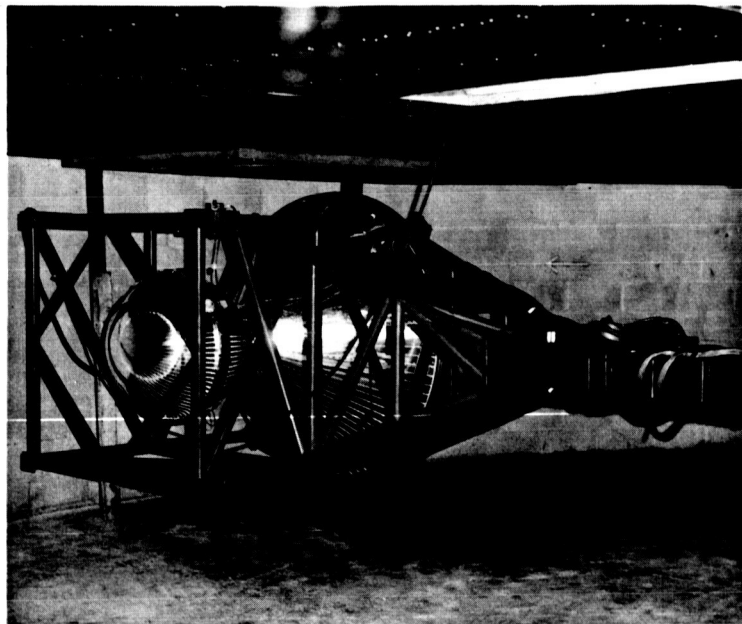
(1) Temperature - 2 channels

(2) Pressure - 2 channels

Figure 17. - Acceleration Test.

48

TABLE V

QUALIFICATION ACCELERATION TEST LEVELS

Axis	Level (g)	Time Duration (minutes)
Longitudinal	11	7
Transverse	2.5	2.5
Lateral	2.5	2.5

TABLE VI

QUALIFICATION TEST LEVEL - STRUCTURAL MARGIN OF SAFETY (M.S.)

(M.S. BASED ON YIELD STRENGTH)

Environment	Location of Max. Stress	Max. Stress (psi)	Yield Stress (Psi)	M.S.
Acceleration	Canister	1060	19,000	16.9
Shock	Canister	710	19,000	25.7
Vibration	Adapter Skin (P axis)	780	38,000	47.7
	Canister (T axis)	505	19,000	36.6
	Canister (N axis)	850	19,000	21.4

(3) The "ejection" indication

(4) Timer (83.5 second contacts)

(5) Timer (90.0 second contacts)

Strain gages were also installed to record canister stresses.

No significant deviation occurred in the output level of either the strain gages or instrumentation subsystem during the test. Additionally, no evidence of damage was found to have occurred as a result of the exposure. It was thereby concluded that the canister assembly and systems would survive stated mission acceleration levels with an adequate margin of safety (Table VI).

The canister assembly was subsequently tested at flight acceptance levels of acceleration (longitudinal axis, 8 g's for 5 minutes) to demonstrate the operational integrity of the prototype inflatable sphere along with the canister assembly and associated systems in a mission environment. The major differences in the tests were that the batteries were excluded and a prototype inflatable sphere was installed. Results obtained during the test show the acceleration environment had no deleterious effects and it was concluded that canister design was adequate. Adequacy of the inflatable sphere design could not be determined at this point in testing since it could not be removed. The inflatable sphere was inspected subsequent to deployment in a 60-foot vacuum chamber.

Vibration tests. - The canister assembly with simulated sphere installed was qualification tested in the required sinusoidal, and random vibration environment (see Figure 18). The sinusoidal vibration test levels are presented in Table VII. The random vibration test levels are shown in Figure 19.
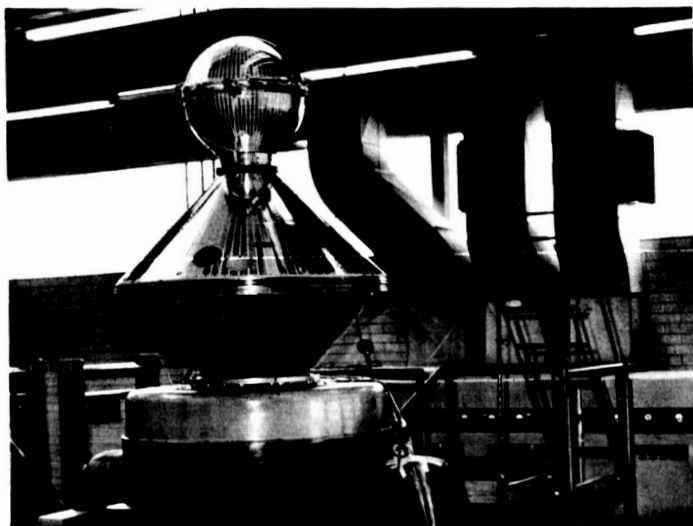

Figure 18. - Vibration Test

TABLE VII

SINUSOIDAL VIBRATION TEST LEVELS   (QUALIFICATION)

Axis	Frequency CPS	Levels
LONGITUDINAL	5-9	$\pm \frac{1}{4}$ in
	9-100	± 2 g
	100-250	± 3 g
	250-2000	± 4 g
*	17-22	± 4 g
TRANSVERSE	5-6	$\pm \frac{1}{4}$ in
AND LATERAL	6-100	± 1 g
	100-250	± 2 g
	250-2000	± 4 g

NOTE: Apply at a constant sweep rate of one octave per minute.
   * Pogo oscillations.

The tests were run to demonstrate that an adequate margin of safety (Table VI) existed throughout the canister assembly and systems to ensure survival when subjected to flight vibrations.

During the tests, power was applied to the flight instrumentation system; the following functions were monitored for performance:

(1) Temperature (2 channels)

(2) Pressure (2 channels)

(3) The "ejection" indication

(4) Timer (83.5 second contacts)

(5) Timer (90.0 second contacts)

In addition, strain gages were used to record canister stresses.

Test results showed that no significant changes occurred in either the instrumentation system or strain gage outputs. However, as a result of the test, a modification was incorporated to add a stiffening shear plate to the timer bracket to avoid undesirable bracket resonance of the timer assemblies.
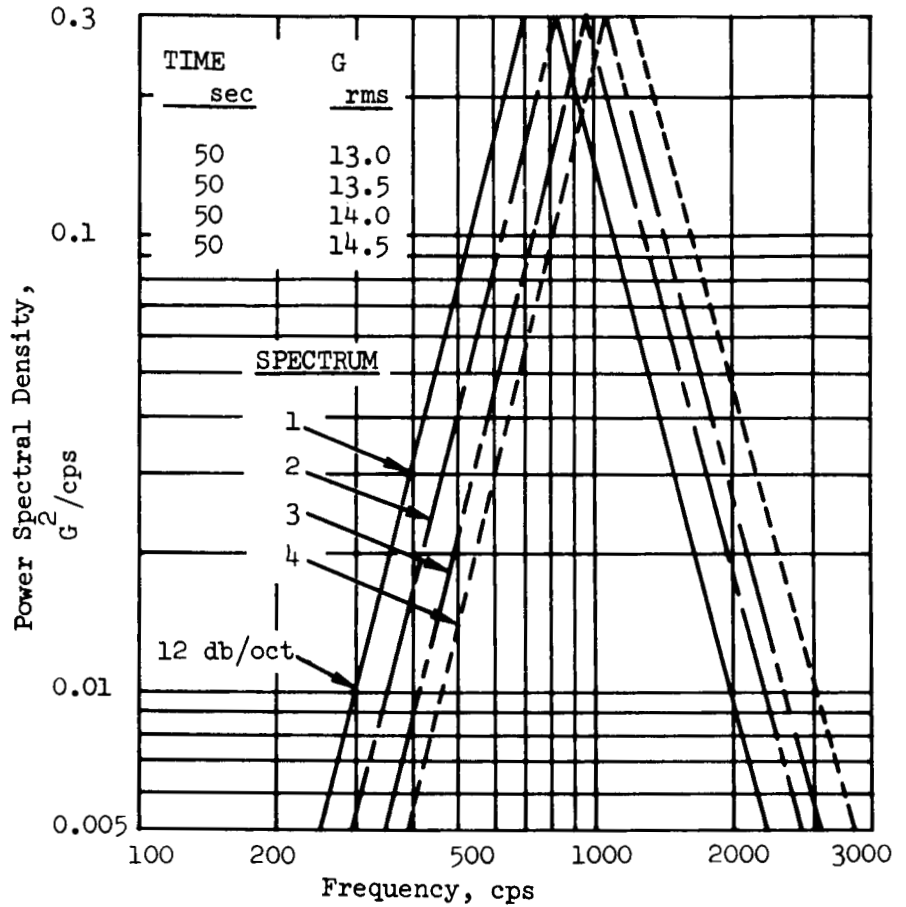
Figure 19. - Random Vibration Test Levels

Upon completion of testing with the above change, it was concluded that the assembly did have adequate margins of safety. The canister was subsequently tested in the longitudinal axis at the flight acceptance levels of vibration (Table VIII and Figure 20). Again, the batteries were excluded and the prototype inflatable sphere was installed. No deleterious effects resulted and it was concluded that the canister design was adequate to survive the mission vibration environment. Again, the inflatable sphere adequacy was to be determined later in the program.

TABLE VIII

SINUSOIDAL VIBRATION TEST (FLIGHT ACCEPTANCE)

Axis	Frequency (cps)	Level
Longitudinal	5-7	$\pm \frac{1}{4}$ in
	7-100	$\pm$ 1.33 g
	100-250	$\pm$ 2.0 g
	250-2000(	$\pm$ 2.67 g
*	17-22	$\pm$ 2.67 g
Transverse	5-100	$\pm$ 0.67 g
and	100-250	$\pm$ 1.33 g
Lateral	250-2000	$\pm$ 2.67 g

* Pogo Oscillations

Note: Apply at a constant sweep rate of
   two octaves per minute.

Shock tests. - Qualification shock tests of the canister was performed with the simulated sphere installed (see Figure 21). Specified levels were applied in the longitudinal axis (15 g's, 6 to 10 ms, half sine wave) to demonstrate that adequate margin of safety (Table VI) exists in the canister assembly and systems to ensure survival through the mission.

Power was applied to the canister instrumentation and the following functions were monitored during the test:

(1) Temperature (2) channels)

(2) Pressure (2 channels)

(3) The "ejection" indication

(4) Timer (83.5 second contacts)

(5) Timer (90.0 second contacts)

Strain gages were again used to determine local stresses.

No significant changes in level of the above signals or in strain gage outputs occurred during the tests. It was concluded that the canister would survive the mission shock environment.
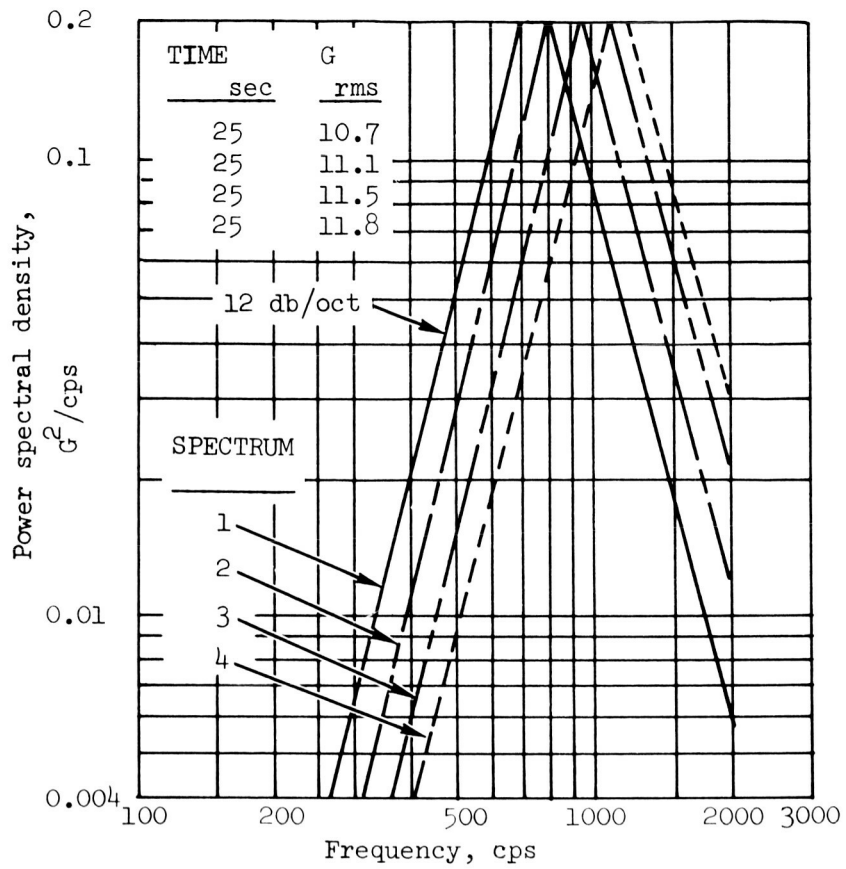
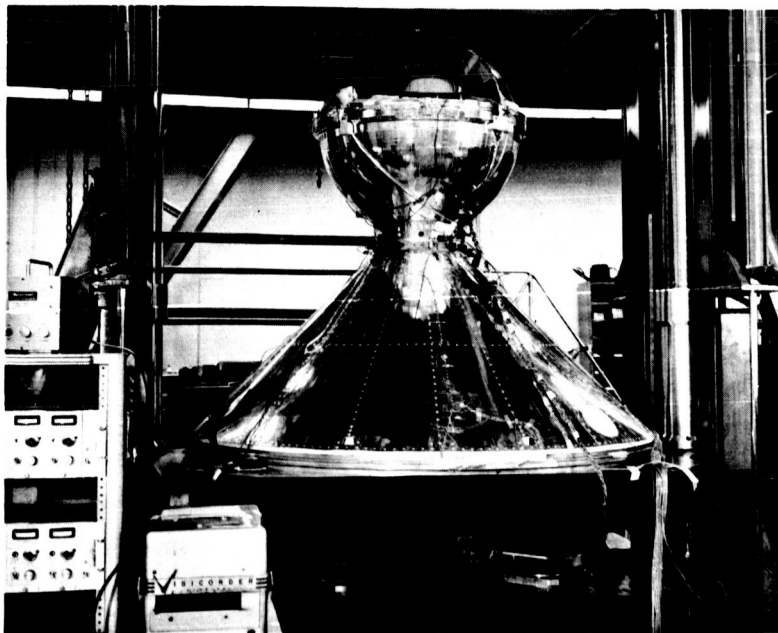Figure 20. - Random Test Levels

Figure 21. - Shock tests.

Noise tests. - Qualification noise tests (see Figure 22) of the canister assembly were performed to demonstrate functional operation of the canister assembly and systems when subjected to the specified noise levels. (Figure 23)

Power was applied to the canister instrumentation and the following functions were monitored during the tests:

(1) Temperature (2 channels)

(2) Pressure (2 channels)

(3) The "ejection" indication

(4) Timer (83.5 second contacts)

(5) Timer (90.0 second contacts)

The recorded levels of the above signals gave no significant change throughout the test. From the test results, it was concluded that the canister assembly would readily survive the mission noise environment.
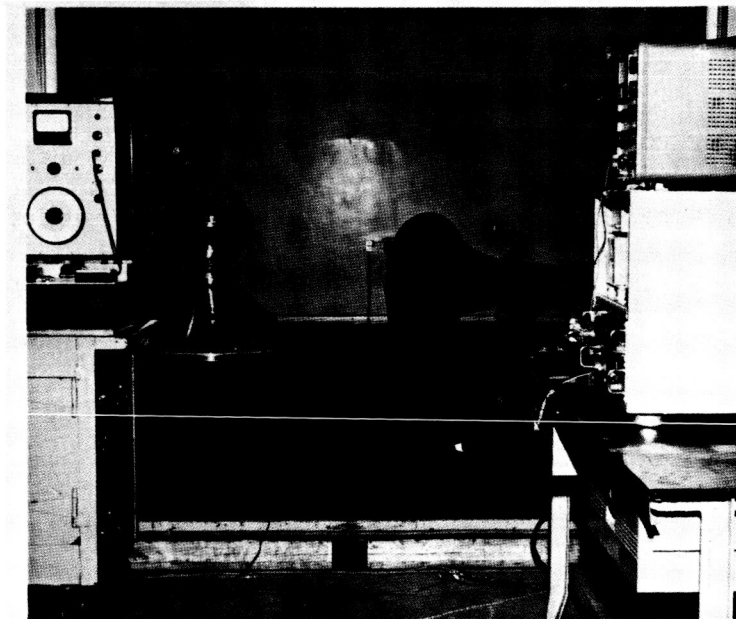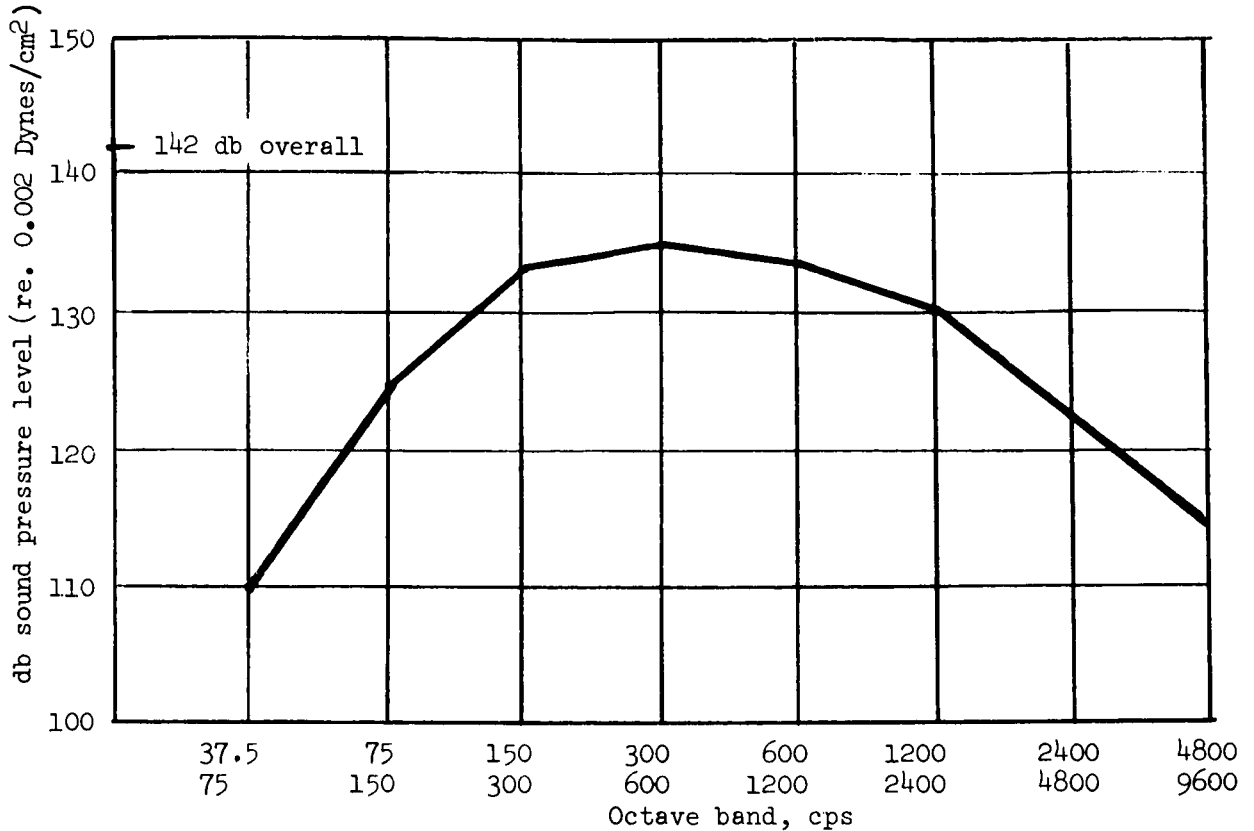

Figure 22. - Noise testing.

Figure 23. - Noise Spectrum

Thermal tests. - Qualification thermal tests (see Figure 24) of the canister assembly with simulated sphere were performed to demonstrate the validity of the thermal balance analysis and the integrity of the canister assembly and systems to this environment. The test was performed in a chamber capable of simulating solar and infrared heating of a specified thermal environment (see Table IX). Twenty-four thermocouples were installed to measure canister surface temperatures at prescribed locations and the following functions were monitored with canister instrumentation power on:

(1) Temperature (2 channels)

(2) Pressure (2 channels)

(3) The "ejection" indication

(4) Timer (83.5 second contacts)

(5) Timer (90.0 second contacts)

Results indicated no unexpected change in level of the above signals. In addition, no damage resulted to the canister assembly and it was concluded

56

that both the assembly and subsystems would adequately survive the mission thermal vacuum environment.

TABLE IX

QUALIFICATION THERMAL TEST LEVELS

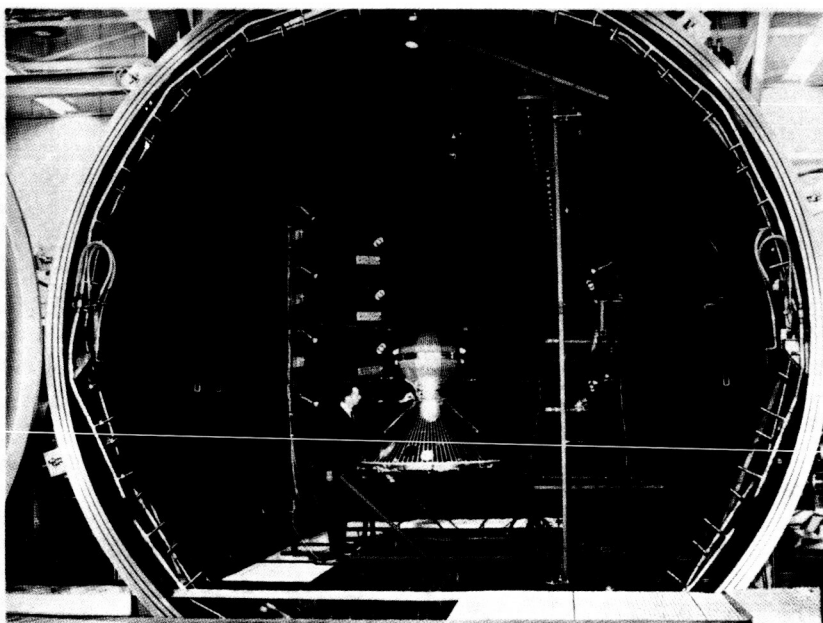| Type	Axis	Direction	Level (Btu/ft^2)	Time (Min)
Solar	x	Normal	440	72
Solar	z	Normal	440	72
Solar	y	Incident (+y)	440	72
IR	x	Normal	110	72
IR	y	Normal	110	72
IR	z	Incident (+z)	110	72

Figure 24. - Thermal testing.

Thermal systems test. - The thermal systems test was conducted after the thermal test and without a sphere in the canister. The test was performed to demonstrate that the canister instrumentation system would perform satisfactorily through the mission thermal environment. For this test, the entire canister assembly was stabilized at 120° F. External power was applied to the canister instrumentation at the ambient and extreme temperatures and the AGE monitor was connected for verification of accuracy and stability of the following functions:

(1) Pressure (1 AGE and 2 telemetry channels)

(2) Temperature (1 AGE and 2 telemetry channels)

In addition, the pressure monitoring channels were checked after 24 hours for repeatibility.

Test results showed that the canister instrumentation was not damaged by the thermal environment and it was concluded that:

(1) The temperature subsystems were sufficiently accurate and stable for the mission.

(2) The pressure systems met the mission accuracy requirements and demonstrated adequate repeatibility when recycled after a longer period than normal to an actual launch.

An anomaly in the pressure data was observed during these tests. The anomaly, which appeared as an increase in pressure, was determined to be a change in gas composition inside the canister. This was a result of outgassing of the anti-chafing liner material during the thermal cycling. This increase, approximately 0.1 torr, was not sufficient to be a problem. Pressure increase due to thermal cycling was found to reduce with liner aging.

Vacuum deployment test. - The deployment test (see Figure 25) using the prototype canister assembly and the prototype inflatable sphere was performed at the LRC 60-foot vacuum facility. The purpose of the test was to prove proper operation of the canister opening system with an actual deployment of the prototype inflatable sphere. The test objectives were as follows:

(1) To demonstrate a minimum of 20 ft/sec separation velocity for the canister halves

(2) Prove integrity of the canister separation joint

(3) Determine inflatable sphere deployment rate

(4) Demonstrate no damage had been sustained by the inflatable sphere by either the opening procedure or simulated flight tests.
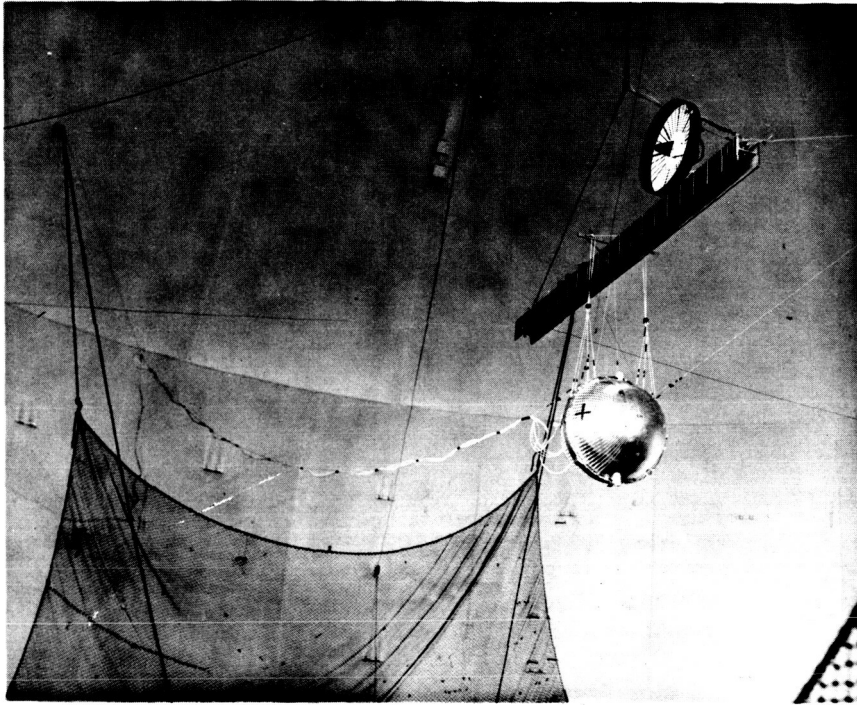
Figure 25. - Deployment testing.

The test was initiated with the canister suspended at the flange lacing thus permitting a free-fall trajectory of the canister halves. Flight battery packs were used to provide power for the canister opening system. Signals representing timer events were recorded to verify the opening system performance. In addition, power was applied to the canister instrumentation system and the following functions were monitored during the test:

(1) Temperature (2 channels)

(2) Pressure (2 channels)

(3) The "ejection" indication

(4) Timer (83.5 second contacts)

Evaluation of test results showed that the velocity of the canister halves was 32.46 ft/sec for the upper half and 27.8 ft/sec for the lower half which was approximately double the deployment rate of the inflatable sphere. The possibility of a space collision by any of the three parts was thereby concluded to be highly improbable. All instrumentation functioned normally and detonation of the shaped charge was through the

timer contacts at approximately 83.0 seconds. The desired "ejection" indication occurred at the 2.0 second timer contact closure. The signal was wired through an adapter located outside the chamber to simulate normal spacecraft airborne operation. Pressures remained nearly constant and temperatures showed an expected 2 to 3° F rise due to the chamber lighting.

Post-test examination of the canister halves revealed minor damage to two fiberglass covers, one of which was later replaced by a coating of RTV compound. Additional changes made at the flange area to provide cleaner separation surfaces were:

(1) All safety wires were coated with RTV.

(2) Solenoid valve covers were trimmed.

(3) Mylar tape covering the shaped charge was cemented in place with a contact cement, (Adhesive EC 1357, 3 M Corporation).

Minor damage to the inflatable sphere was later attributed to the test configuration and not considered significant to the extent of requiring further changes or retest. In general, the test was considered success and it was determined that the mission could be performed with the existing opening system configuration.

Dimple motor tests. - Qualification tests of the DM25N4 dimple motors included vibration and thermal environment tests and RF suscepti- bility tests. The twofold purpose of testing was:

(1) Verify performance of the units operationally after being subjected to the simulated vibration and thermal environments.

(2) Verify that RF levels of 28 volts per meter for frequencies below 50 mc, and 194 volts per meter for frequencies above 50 mc would not cause an unexpected firing of the dimple motors individually, when installed in flight timer assemblies, or in the operational configuration.

During thermal and vibration environmental exposures, bridge resistance was monitored and found to have no substantial change. Further results in the tests showed that:

(1) The dimple motors functioned normally after the vibration and thermal tests.

(2) The dimple motors survived the three phases of RF exposure with no deleterious effects.

It was concluded that the dimple motors would not be effected by mission RF exposures and would perform satisfactorily after exposure to mission vibration and thermal environments.

Flight Acceptance Test Program

The objective of the Flight Acceptance Test Program (FAT) was to verify the integrity of the components and the quality of workmanship employed in the construction of the flight spacecrafts.

In order to accomplish this purpose, each flight spacecraft was subjected to the same series of simulated flight environments and the performance of the spacecraft measured before, during or after each environmental exposure.

Procedures. - The acceptance tests were similar in nature to the qualification tests. Identical functions of the instrumentation system were monitored during each test. Each flight unit was tested in four environments (vibration, acceleration, shock, and thermal) as follows:

(1) Vibration - random and sinusoidal (Table VIII and Figure 20)

(2) Acceleration - 3 axes (Table X)

(3) Shock - thrust axis (12 g's for 6 to 10 ms, half sine wave)

(4) Thermal - instrumentation ($120 ^{+2}_{-0}$ degrees F for 72 minutes)

In addition, a systems test was performed following the acceptance test to verify that the canister opening and ejection systems had survived without damage.

Results. - The test results showed no significant deviation in the monitored signals. The subsequent visual inspection and system test were satisfactorily completed with no evidence of structural or component damage.

TABLE X

FLIGHT ACCEPTANCE ACCELERATION TEST LEVEL

Axis	Level (g's)	Time Duration (Min)
Longitudinal	8	5
Lateral	2	2
Transverse	2	2

CONCLUSIONS

The requirements for the canister assembly, as shown in the design constraints, were all achieved. To obtain the minimum canister half opening velocity of 20 ft/sec, a nominal charge of 40 grains per foot was required. The 40 grain charge produced a velocity between 26 to 29 ft/sec. The effect of blast did not cause any cracks at the flanges.

The canister opening between 60 and 90 seconds after separation from the launch vehicle was controlled by setting the primary timer at 83.5 seconds and the secondary timer at 90 seconds.

The ejection velocity of 6 ft/sec-minimum was achieved by the ejection spring design. When tested during free drop, a velocity of 8.12 ft/sec was attained when both bolts were exploded, and 7.79 ft/sec when one bolt was exploded.

The anti-chafing liner was a Teflon material (known as Emerlon 320) and was the same material as was used in the Echo II canisters. It was determined during the Instrumentation Thermal Test that this material out-gassed when the canister temperature was raised from 80° F to 120° F and that, when the canister was returned to 80° F, there was some recondensing of the products that out-gassed. The material functioned very satisfactorily as an anti-chafing liner.

The thermal protective materials used, functioned satisfactorily. The results of the flight temperatures (not included in this report) are expected to be within limits since the analysis was conservative due to the balloon not being included in the analysis. The balloon has a moderating effect on both the heat gain and heat loss. The analysis required the female or bottom flange to be approximately 5° F warmer than the top or male flange. This was done to assure that there would be no tendency for seizure between the sliding valve portion of the flanges due to temperature changes during flight and prior to canister opening.

There was no difficulty experienced in meeting the leak rate of 0.1 torr per 24 hours except when accompanied by temperature changes. When the canisters were in a constant temperature environment, there was little pressure change (0.008 torr for 24-hour period).

The canister assembly weight of 95 lbs. and the 265 total maximum weight of the canister plus the inflatable sphere assembly were achieved with some margin. The canister assembly weights varied from 90.42 lbs. to 92.10 lbs. Canister assembly No. 3, with the inflatable sphere, weighed 238.30 lbs. and canister assembly No. 4, with the sphere, weighed 240.27 lbs.

The spacecraft was successfully launched into orbit from the Air Force Western Test Range on 23 June 1966 with all spacecraft functions performing nominally.

LIST OF REFERENCES

1. GER-10946: "Satellite Radiation Heat Balance Program." Akron, Ohio, Goodyear Aerospace Corporation, 10 January 1963.

2. GER-11618: "Albedo Radiation on a Sphere or Planet-Oriented Flat Plate." Akron, Ohio, Goodyear Aerospace Corporation, July 1964.

3. Scalan, R. H. and Rosenbaum, R.; Introduction to the Study of Aircraft Vibration and Flutter. McGraw-Hill Book Company, Inc., New York, N.Y. First printing, 1951.

4. Jacobsen, L. S. and Ayre, R. S.; Engineering Vibrations. McGraw-Hill Book Company, Inc., New York, N.Y., 1958.

"The aeronautical and space activities of the United States shall be conducted so as to contribute . . . to the expansion of human knowledge of phenomena in the atmosphere and space. The Administration shall provide for the widest practicable and appropriate dissemination of information concerning its activities and the results thereof."

—NATIONAL AERONAUTICS AND SPACE ACT OF 1958

NASA SCIENTIFIC AND TECHNICAL PUBLICATIONS

TECHNICAL REPORTS: Scientific and technical information considered important, complete, and a lasting contribution to existing knowledge.

TECHNICAL NOTES: Information less broad in scope but nevertheless of importance as a contribution to existing knowledge.

TECHNICAL MEMORANDUMS: Information receiving limited distribution because of preliminary data, security classification, or other reasons.

CONTRACTOR REPORTS: Technical information generated in connection with a NASA contract or grant and released under NASA auspices.

TECHNICAL TRANSLATIONS: Information published in a foreign language considered to merit NASA distribution in English.

TECHNICAL REPRINTS: Information derived from NASA activities and initially published in the form of journal articles.

SPECIAL PUBLICATIONS: Information derived from or of value to NASA activities but not necessarily reporting the results of individual NASA-programmed scientific efforts. Publications include conference proceedings, monographs, data compilations, handbooks, sourcebooks, and special bibliographies.

Details on the availability of these publications may be obtained from:

SCIENTIFIC AND TECHNICAL INFORMATION DIVISION

NATIONAL AERONAUTICS AND SPACE ADMINISTRATION

Washington, D.C. 20546